B140020
Improved construction of roads and pipelines to minimize impact on peatland greenhouse gas emissions

Maria Strack
Department of Geography, University of Calgary
2500 University Dr NW, Calgary, AB T2N 1N4

Project advisor: Brett Purdy

Completion date: January 15, 2019

Submitted: April 15, 2019

Prepared by: Maria Strack, Mustafiz Rahman, Greg McDermid, Bin Xu, Julie Lovitt, Annie He and Saraswati Saraswati

Table of Contents

List of Figures

List of Tables

Executive Summary

In partnership with Emissions Reduction Alberta, Shell Canada Ltd. and Canadian Natural Resources Ltd., this study investigated the potential of culverts installed in permanent linear disturbances (in this case access roads) to mitigate greenhouse gas (GHG) emissions from peatland ecosystem. Northern peatlands are globally significant carbon sinks and sources of methane (CH_4). While many reports of hydrological impacts related to road crossings in peatlands have been reported, no previous studies have quantified the effect of this disturbance type on GHG emissions, nor the potential of culverts to mitigate the impact. In order to determine both road impact and mitigation potential of culverts, we sampled local GHG flux in summer 2016 and 2017 in both a bog and fen peatland near Peace River, AB. At each peatland, measurements were made along triplicate transects running perpendicular to the road that were at least 20 m away from a culvert and at an additional set of triplicate transects located within 2 m of the culvert. The road impact was determined by comparing the transect far from culverts to control plots located greater than 50 m from the road. The effect of the culverts was determined as the difference between transects close and far from culverts. In order to better map linear disturbance impacts across the landscape, we also developed a series of geospatial tools, largely using unmanned aerial vehicles (UAVs), for evaluating hydrological and ecological conditions in boreal peatland ecosystems. Finally, as road crossings were co-located with seismic lines, we used this study as an opportunity to investigate their potential impact on peatland CH_4 emissions.

We successfully mapped microtopography, water table position in a bog, and shrubby biomass in fens using UAV photogrammetry. Using these results were evaluated the impact of low impact seismic lines on peatland microtopography and CH_4 emissions. Water table position is shallower, hummock coverage is lower and CH_4 emissions likely elevated on low impact seismic lines. Extrapolating these results to the total seismic line length in Alberta's peatlands suggested that these disturbances may results in an additional 4.1 to 5.0 kT of CH_4 emission from peatlands annually.

The road crossing resulted in substantial hydrological impact at our bog study site, but not at the fen. This was attributed by the direction of the road crossing relative to the local slope. Slope was minimal at the fen and the road was nearly parallel to the slope, limiting hydrologic impact. At the bog, culverts mitigated some of the hydrologic impact, but were spaced too far apart to reduce flooding on the upgradient side. Results indicate that for this site, culvert spacing would need to be less than 20 m to be effective. At both study sites, the road resulted in reduced GHG uptake, although on average across the area extending 40 m from the road on both sides, both sites remained GHG sinks. At the fen, reduced plant productivity led to a reduction of GHG uptake of $180 - 330$ g CO_2-e m^{-2} yr^{-1}. At the bog, GHG uptake was reduced by $600 - 900$ g CO_2-e m^{-2} yr^{-1}, both due to lower CO_2 uptake and greater CH_4 emission. Culverts did not mitigate the road impact and, in fact, appeared to strengthen it at this study site.

Future research should focus on road construction designs that enable dispersed hydrologic connection and the effectiveness of these to reduce GHG impact in peatlands. Future studies should also aim to utilize the geospatial tools developed here to map linear disturbance impacts across a wider range of peatland types and time since disturbance to better quantify GHG impacts in peatlands across regional to provincial scales.

1. Project Description

Peatlands are abundant in Alberta, covering approximately 16% of the province's land area. In Alberta's boreal zone, peatland coverage is up to 70% in some regions. Thus, the development of oil sands resources – also largely located in the province's boreal region – has the potential to disturb a large area of peatland through mining and well-pad construction, exploration lines, roads and pipelines. Flooding and tree mortality are often observed adjacent to road crossings in wetlands. Although a variety of alternative construction methods have been suggested, there is little motivation to implement these methods as their benefits remain unclear.

Given that peatlands are globally significant stocks of soil carbon and a source of methane, hydrological disturbances will contribute to significant land-use change greenhouse gas (GHG) emissions. The importance of GHG emissions associated with wetland land use change and management has been highlighted by the recent adoption of the Wetland Supplement, which provides guidance for estimating emissions and removals from wetlands in national GHG inventories (IPCC, 2014). This project focused on minimizing the GHG emissions related to the construction of linear disturbances that involve the placement of mineral soil fill on peatlands during construction. Since these roads will remain, in most cases, in place for decades, we refer to these as "permanent" linear disturbances (PLD). Documenting GHG reduction opportunities related to construction methods of PLD will provide motivation for operators to implement these methods in order to reduce costs of future reclamation and obtain GHG offset credits.

The original objectives of the project were: 1) to determine the impact of current PLD on peatland GHG emissions and 2) to evaluate innovative, low-impact methods of construction for reduction of GHG emissions related to disturbance. Our goal was to measure the GHG impacts at local study sites and develop geospatial methods that could map these impacts across larger areas. Due to closure of the in situ oil sands site where the work was conducted, we were unable to design new PLD segments implemented with innovative construction. Instead, we utilized existing PLD (road) segments with culverts placed 50 m apart and sampled close and far from culverts to evaluate the ability of culverts is reduce GHG emission impacts of the PLD. Additionally, during image analysis of the data collected with a small unmanned aerial vehicle (UAV) to map changes in water table position related to PLD, we recognized the potential to map seismic line impact to peatland GHG emissions. Therefore, we also added an objective to 3) evaluate the local and provincial impact of seismic lines on peatland methane (CH_4) emissions.

We chose to focus on access roads in our study of PLD in peatlands given the difficulty of working near pipelines. We instrumented segments of roads that crossed a shrubby rich fen and a treed bog near Peace River, AB. At each road site, we installed three transects close to (<2 m) culverts and three transects far from (>20 m) culverts. Along each transect, GHG flux sampling plots were installed at 2, 6 and 20 m from the road on both the upgradient and downgradient sides. We also installed at least three additional plots 50 m from the road (six were used at the bog site) for use as undisturbed plots. This resulted in 39 plots at the fen and 42 plots at the bog site. At each of these plots, GHG flux measurements were made at least biweekly between May and August in 2016 and 2017, with additional winter measurements in winter 2015-2016. Near each plot we also measured water table position, soil temperature, ground layer plant cover and biomass, overstory biomass and net primary production and soil phenolic compound concentration and extracellular

enzyme activity. Photogrammetry data was collected using a UAV over a 1 km by 1 km area surrounding the road at both the fen and bog. Imagery was collected at both sites in June and August, 2016, at the fen in May 2017 and in a smaller areas close to the road (~200 m) at bog sites in August 2017. These data, along with satellite imagery were used to evaluate slope, microtopography, water table position, land cover type and overstory biomass across the study areas and upscale GHG estimates from the plot scale study to the entire road impacted area.

2. Outcomes and Learnings

Outcomes of research completed as part of the project are detailed in project summaries below. These directly relate to the project objectives set out in the original proposal and also include additional work that was possible due to this funding in relation to the GHG impact of peatland seismic lines. We start with projects related to the development of geospatial tools to map the impacts of PLD (roads in this case) relevant for GHG estimation (microtopography, land cover, water table, biomass) and follow with direct measurement of hydrological and biogeochemical impacts measured at our study sites.

2.1. Mapping shrub biomass in a boreal continental fen

Biomass estimation is a commonly explored topic in the literature; however, the application of these methods in peatlands is limited. Since plants facilitate carbon storage through photosynthesis, vegetation-biomass estimates are necessary for calculating carbon budgets and are a key element of carbon-dynamics models. Shrubs can be a dominant vegetation type found in peatlands, specifically in boreal continental fens. Biomass estimation includes above and below-ground biomass, however, our study focused solely on aboveground biomass (AGB). In this study, two methods will be used to estimate shrub biomass in a boreal continental fen located in Northern Alberta. The first objective is to develop allometric equations for the dominant shrub genera. Allometry is a popular field-based method commonly used for biomass estimation. Allometric equations use one or more plant dimensions to estimate a separate dimension that is more difficult to obtain (e.g. biomass). The second objective is to assess the potential of using unmanned aerial vehicles (UAV) to estimate biomass of the entire study site. Shrubs are typically multi-stemmed and are relatively small in size, which poses challenges in detection through remote sensing platforms. We believe that UAVs offer the sufficient spatial resolution to capture the small-stature vegetation that can dominate some peatlands. This is the first known study that has used UAVs to map shrub biomass in a boreal continental fen.

Experimental procedures/methodology
Allometric study:
We harvested a total of 82 stems of the three dominant genera to be used to develop the allometric models. Basal diameter, the stem diameter at 15 cm above the ground, was used as the predictor variable for our allometric equations. IBM's SPSS statistical software was used to fit a power regression line for each genus and we also developed a generalized equation that included all samples (not separated by genus).

UAV study:

We destructively harvested 30 shrubs in a boreal continental fen in Northern Alberta. The field samples were used as calibration and validation data for the development of the shrub biomass map. Sensefly's eBee was the UAV used to conduct two UAV flights to obtain Leaf-on and Leaf-off data. From these two datasets, we are able to generate a canopy height model which was used to obtain structural variables. We tested the performance of spectral variables (e.g. vegetation indices) and the structural variables (e.g. shrub height, shrub volume, etc.) in predicting aboveground biomass. The best predictor variable was used for the UAV-biomass regression and applied to all shrubs found in the study site.

Results and discussion

Allometric Study:

Table 1 summarizes the results for the allometric study. We found that basal diameter (stem diameter at 15 cm above base of stem) was a good predictor of AGB. All phylogenetic equations had a $R^2 > 0.9$. We also found that the generalized equation was not significantly from any of the phylogenetic equations.

This indicates that phylogenetic equations are not required to obtain accurate biomass estimates.

Table 1: Summary of the allometric equations relating basal diameter to aboveground biomass, including coefficients of determination (R^2). The reported n represents number of stems. The sample size (n) is the number of stems used to develop each regression. T-values represent differences in y-intercept (a) and slope (b) from that of the general equation, and include p-values. Those differences that are significant at the 0.05 threshold are marked as *.

	n	*a*	*b*	*R^2*	*a* Test-*t*-Value (*p*)	*b* Test-*t*-Value (*p*)
Phylogenetic Equations						
Alnus	27	44.06	2.395	0.98	1.83 (0.07)	1.83 (0.07)
Salix	49	55.85	2.325	0.94	0.94 (0.35)	1.56 (0.12)
Betula	25	49.52	2.027	0.91	0.19 (0.85)	0.77 (0.44)
Alnus & Salix	76	52.88	2.291	0.96	0.44 (0.66)	0.56 (0.57)
General Equation						
General	82	53.37	2.251	0.97	N/A	N/A

UAV study:

Table 2 summarizes the performance of each variable with AGB. Within the field data variables, height ($R^2=0.705$) performed better than width ($R^2=0.417$). Height and width were then fit into a multiple regression equation, which produced an adjusted R^2 value is 0.74 and RMSE of 744.336 g. The adjusted R^2 was used, as opposed to the R^2, because it accounts for the addition of a variable. Both variables were found to be statistically significant (p<0.01). Height from the field and from UAV performed similarly with R^2 values of 0.705 and 0.713, respectively.

Amongst the UAV-structural variables, volume ($R^2=0.885$) performed the best and mean height performed the worst ($R^2=0.594$). The four spectral variables all had a R^2 of less than 0.27 with the Simple Ratio VI performing the best ($R^2=0.274$). The results from Table 2 concludes that the UAV-structural variables performed better than the spectral variables. UAV-volume had the lowest RMSE and highest R^2, overall, therefore it was used as the predictor for our AGB equation.

Table 2: A summary of each model's performance with dried aboveground biomass based on coefficients of determination (R^2) and root-mean-square errors (RMSE). The * indicates that an adjusted R^2 was reported because a multiple linear regression was used instead of a simple linear regression.

	R^2	RMSE(g)
Field Data		
Height	0.705	802.359
Width	0.417	1126.763
Height & Width	0.740*	744.336
UAV – Structural Variables		
Max height	0.713	790.26
Volume	0.885	500.33
Mean height	0.594	940.56
UAV – Spectral Variables		
Red Edge	0.004	1473.67
NDVI	0.116	1388.29
Red Band	0.21	1312.01
RVI/ Simple Ratio	0.274	1257.95

The linear regression equation coefficients (derived from UAV based shrub volume measurements) are reported in Table 3.

Table 3: Model parameters for AGB linear regression with UAV-volume as the predictor variable. Standard error of the slope coefficient (b) and constant (a) are reported with the mean average error (MAE).

b	SE[b]	a	SE[a]	MAE(g)
0.5776	0.04	507.34	112.11	421.05

The equation was applied to all shrub objects across the site. Table 4 summarizes the descriptive statistics for shrub objects. There was a total of 70793 shrub objects and the average size of each shrub (in pixels) is approximately 388. The smallest shrub object covered 111 pixels and the largest shrub covered 3574 pixels. AGB ranged from 52.5 g to 6396.5 g and the average biomass per shrub was 760.7 g.

Table 4: Descriptive statistics for shrub objects. N is the number of shrub objects in the study site. Biomass in this table refers to aboveground biomass.

	N	Average size (pixels)	Minimum Size (pixels)	Maximum size (pixels)	Minimum biomass (g)	Maximum biomass (g)	Average biomass (g)	Total Biomass (kg)
Shrubs	70793	388	111	3574	52.5	6396.5	760.7	53854.2

The total AGB (dry weight) was calculated as 53 854.2 kg (Table 4 and Figure 1). We were unable to harvest shrubs that could be used as a quantitative measurement of the map's accuracy; however, we believe the cross-validation of the volumetric equation is sufficient in assessing the accuracy of the AGB map.

Lessons learned
Allometric Study:
Through this study, we developed 3 phylogenetic equations for peatland shrub species that did not previously exist in the allometric literature. We also demonstrated that a generalized equation for the three dominant shrub species (*Alnus, Betula, and Salix*) was not significantly different than each phylogenetic equation. The discussion of generalization of allometric equation is common in the literature and our findings contribute to this body of research.

Dried Aboveground Biomass (g)
Value
High - 6396 g
Low - 0 g
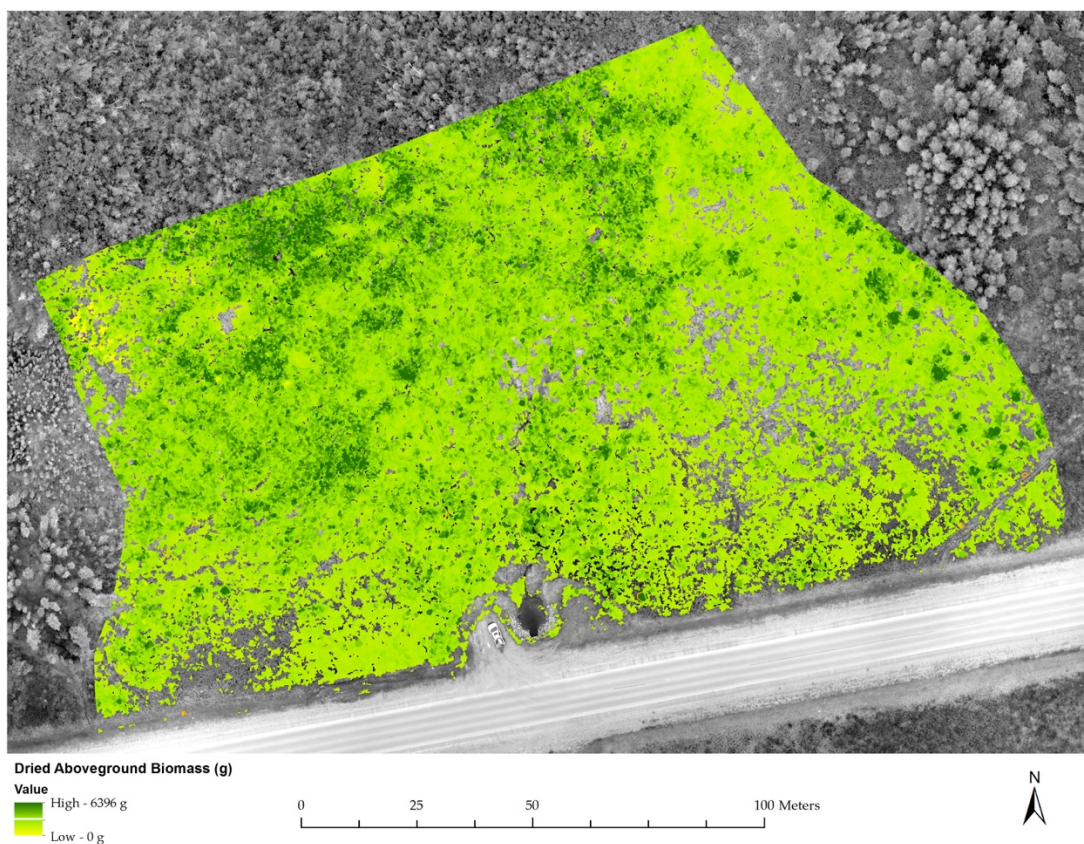
Figure 1: Aboveground biomass (AGB) map generated based on a simple linear regression model with UAV-volume as the predictor. The estimated dried weight of AGB across this site is 53 854.2kg. The underlying image is an orthoimage of the study site.

UAV Study:

This study is the first biomass estimation study undertaken in peatlands using UAVs. We have demonstrated that UAVs are not only able to capture low stature shrubs (< 1 m in height) but that they can be used to estimate individual shrub biomass using volumetric information. The UAV platform was able to offer the high-resolution imagery required to face the challenges associated with mapping low-lying shrubs. Our site had the additional advantage of only being composed of three dominant shrub species which had also been found, in a previous research paper, to not be structurally different from each other. Other researchers that use this method may have the additional challenge of having to identify species and applying species-specific equations.

2.2. A method for shadow removal in UAV data

Shadows from clouds, trees, buildings, and other elevated features are present in most remote sensing imagery. While shadows can play a key role in image interpretation (e.g. Lillesand et al. 2008) and object detection (e.g. Tong et al. 2013), they are most often viewed as noise: regions *impaired data* or *no data* that hinder a broad range of image-processing routines (Saha et al. 2005; Li et al. 2014). While shadows are present in optical data acquired from all platforms (ground, airborne, and satellites), they are perhaps most problematic in high-spatial-resolution airborne imagery (Liu and Yamazaki 2012), such as those collected from unmanned aerial vehicles (UAVs). In this study, we propose a new UAV-based data collection and processing workflow designed to produce seamless, shadow-free orthomosaics. We demonstrate our techniques over a ~700 m X 700 m treed bog site in Northern Alberta (Figure 2).
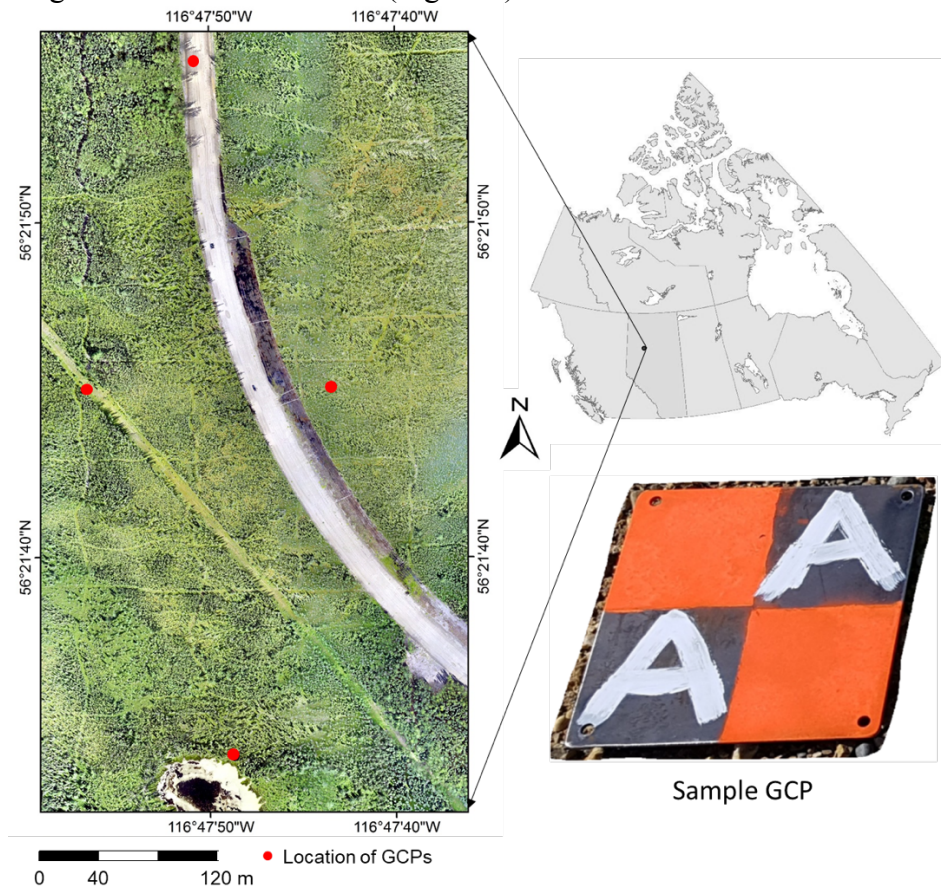
Figure 2: Location and overview of the study area in Northwestern Alberta, Canada.

Methods

Our workflow for reducing shadow in UAV-based orthomosaics is comprised of three stages: (i) image acquisition, (ii) shadow detection, and (iii) shadow-masked orthomosaicking (Figure 3). Each of these stages is described below.

Shadow Detection

Generate 3D surface model of study area

Orthorectify individual photographs

Create binary shadow/no-shadow model of each orthophoto

Image Acquisition

Two data sets with diverging shadow orientations: before and after solar noon

Shadow-Masked Orthomosaicking

Mask shadow based on the shadow/no-shadow model

Create orthomosaic using shadow masked photographs

Figure 3: A workflow for creating shadow-reduced orthomosaics from two-pass UAV photography.

Results and discussion

To evaluate the performance of our workflow, we compared a shadow-reduced orthomosaic to a traditional one obtained from a single flight. A qualitative assessment of the corresponding data products reveals the visual efficiency with which shadows have been eliminated (Figure 4), to the point where some ground features (trees, for example) are difficult to identify without their corresponding shadows. The performance of the workflow was confirmed with a quantitative assessment, wherein we classified the raw orthomosaic into two classes – *shadow* and *other* – using an unsupervised (K-Means) decision rule. An assessment of the accuracy of this classification was performed using randomly selected *shadow* (70 nos.) and *other* class sample points (70 nos.). The reported classification accuracy was 96% with a kappa of 0.91. According to our classification, 22.3% of the study area was covered by shadow in the raw orthomosaic. From a visual assessment, a complete lack of shadow was observed on the shadow treated orthomosaic. The following sections briefly describe how the shadow-treated orthomosaic performed under different conditions.

Compensating for shadows using multi-temporal imagery is normally constrained by three main factors: (i) geometric mismatch, (ii) radiometric mismatch, and (iii) cost. Our workflow using multi-flight UAV data minimizes the influence of all three factors. For example, image mosaicking is traditionally performed using a *superimposing* method (Rahman et al. 2013), based on geometric location of individual pixels within the photos or scenes. This strategy focuses geometric distortion (caused primarily by errors in the GCPs and georeferencing model) along seam lines. By contrast, the high overlap (60-90%) delivered by UAV flights permits the use of a *feature-matching*

8

mosaicking strategy. Feature matching identifies distinct features within the photos and uses their relative location to warp and mosaic them together. As a result, the final product is seamless. Compensation for shadows using multitemporal imagery is usually done with historical data, with images acquired from a different date. Consequently, the radiometry among image dates is expected to vary due to phenological changes, varied sun-surface-sensor geometry, and environmental conditions, making it difficult to produce a seamless mosaic. In contrast, UAV platforms are able to collect data quickly and repeatedly, delivering data with similar illumination conditions and same-day target status.

It is perhaps unfair to compare the cost of piloted aircraft or satellite platforms to that of a UAV. However, the negligible set-up and operating cost of a UAV system allows for rapid, repetitive, and on-demand data collection to meet the needs of producing high-quality, shadow-free orthomosaics.

Lessons learned

Our straightforward workflow capitalizes on the strengths and flexibility of the UAV platform, and is capable of detecting and reliably compensating for shadows across a vegetated study area. We characterize the shadow in our study area as complex, since their size, shape, and orientation varies abruptly. We look forward to future applications of this workflow to other natural and urban settings.

	With Shadow	Without Shadow
Mineral Road		
Seismic Line		
Disperse Canopy		
Dense Canopy		
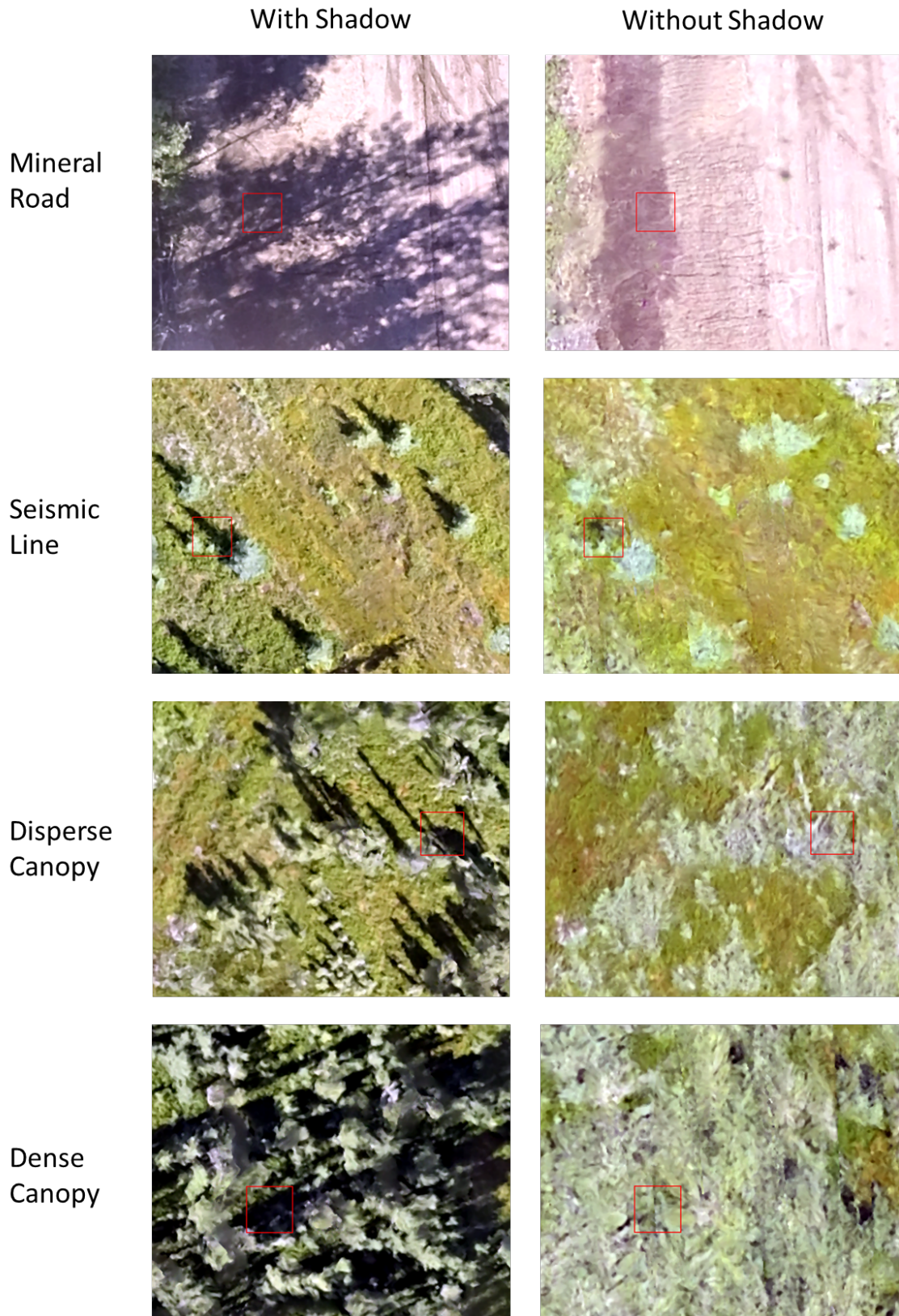
Figure 4: A visual comparison of shadow-reduced (right) and raw (left) orthomosaics of scenes within the study area.

2.3. The influence of surface complexity on UAV point cloud elevation accuracies in modeling peatland microtopography

Fine-scale ground surface heterogeneities (microtopography) are an important controlling factor of peatland greenhouse gas (GHG) distribution and flux (Cresto Aleina et al., 2015), and have been shown to improve carbon balance model accuracies when included (Shi et al., 2015; Strack et al., 2006). Previous research shows these data have been successfully collected with high accuracy via unmanned aerial vehicles (UAVs) in open peatlands (Lehmann et al., 2016; Lucieer et al., 2014). However it is unknown how the increased surface complexity of treed bogs, common to western Canada, will impact UAV point cloud performance. In this case surface complexity refers to a combination of vegetation/canopy cover, surface roughness and the degree of spectral homogeneity.

The objectives of the study were (i) to assess UAV photogrammetry for capturing ground surfaces in peatlands of varying complexity: from relatively flat, open areas to a mixture of highly undulating (rough) and treed zones. Our goal is to determine the conditions under which UAV photogrammetry can accurately detect ground-surface elevation: paving the way for future work on micro-topographic mapping, and (ii) to describe the value of supplementing LiDAR with UAV data in estimating ground surfaces over varying degrees of surface complexity.

Methods

This project aims to assess the capability of UAV photogrammetry for capturing ground surfaces in a peatland under varied surface complexity, and to display the potential benefits of supplementing existing LiDAR with UAV data. To meet the first objective, a set of UAV photos were collected and processed to generate a photogrammetric dense point cloud. Then, the ground was extracted from the dense point cloud to model the terrain. A set of (678 nos) field data (RTK) points were collected across the study site to evaluate the performance of the terrain model under different surface complexity; 0. Bare Areas (newly constructed roadway), 1. Low complexity (disturbed peatland areas along pipelines, seismic lines etc.), 2. Moderate complexity (undisturbed areas with Labrador Tea and/or sparse trees), and 3. High complexity (undisturbed, potentially densely treed areas with limited ground visibility). To attain the second objective, a set of LiDAR data (ground points) was used to model the terrain. Then, another terrain model was created by combining the LiDAR based- and UAV based- ground points together. These two models are then compared under different surface complexity. The study site for this research is a ~1km x ~1km section of a treed bog located within the Shell-Carmon Creek development area, approximately 35km northeast of Peace River, AB, Canada.

Results and discussion

Results of the two rigorous elevation accuracy assessments, involving assessment of all 678 RTK points and assessment of classified RTK points, are summarized in Tables 5 and 6 below. Table 1 displays dataset accuracies of all 678 RTK points while Table 6 displays accuracies for points grouped by surface complexity.

Table 5: UAV Dataset Accuracies: Comparison of Dataset Elevations against all 678 RTK Surveyed Point Elevations

Dataset	Average Absolute Error (m)	Mean Error (m)	RMSE	Median Error (m)	Median Offset (m)
UAV	0.31	0.27	0.40	0.25	0.23

Table 6: UAV Dataset Accuracies: Comparison of Dataset Elevations against RTK Point Elevations Classified by Surface Complexity

Surface Complexity Class	Average ABS z Error (m)	Mean Error (m)	RMSE	Median z Error (m)	Median Offset (m)
Bare Areas (42 points)	0.14	-0.01	0.15	-0.08	-0.10
Class 1 (53 points)	0.21	0.15	0.26	0.15	-0.10
Class 2 (264 points)	0.23	0.21	0.28	0.20	0.15
Class 3 (319 points)	0.42	0.37	0.51	0.35	0.47

Since the variance and sample size of these data were unequal, a robust one-way analysis of variance (ANOVA) and Welch's test were conducted in SPSS software to determine whether significant differences existed between classes of surface complexity ($\alpha=0.05$). Results indicated statistically significant differences did exist between classes (ANOVA: $F_{(3,674)}=36.969$, $p<0.001$, Welch: $F_{(3, 134.225)} =53.185$, $p<0.001$). A post-hoc Tamhane pairwise comparison ($\alpha=0.05$) revealed Class 0 and 3 were significantly different from other classes, with all $p<0.001$, however Class 1 and 2 are not significantly different from each other ($p=0.381$). A non-parametric Kruskal Wallace test corroborated these findings.

Results of the elevation accuracy assessments to evaluate the value of adding LiDAR are provided in Tables 7 and 8 below. Table 7 summarizes dataset performance across all suitable 629 RTK points, while Table 8 displays elevation accuracies of points classified by surface complexity.

Table 7: LiDAR and Supplemented LiDAR Dataset Accuracies: Comparison of Dataset Elevations against all 629 RTK Surveyed Point Elevations

Dataset	Average Absolute Error (m)	Mean Error (m)	RMSE	Median Error (m)	Median Offset (m)
LiDAR	0.42	0.41	0.84	0.25	0.47
LiDAR+UAV	0.30	0.27	0.38	0.25	0.27

Table 8: LiDAR and Supplemented LiDAR Dataset Accuracies: Comparison of Dataset Elevations against RTK Point Elevations Classified by Surface Complexity

	Dataset	Average ABS z Error (m)	Mean Error (m)	RMSE	Median z Error (m)	Median Offset (m)
Class 1	LiDAR	0.14	0.12	0.18	0.10	-0.01
(53 points)	UAV + LiDAR	0.20	0.14	0.25	0.14	-0.06
Class 2	LiDAR	0.34	0.33	0.68	0.23	0.33
(264 points)	UAV + LiDAR	0.23	0.21	0.27	0.20	0.15
Class 3	LiDAR	0.58	0.56	1.10	0.29	0.56
(312 points)	UAV + LiDAR	0.39	0.35	0.47	0.32	0.46

A two-way mixed model ANOVA test ($\alpha=0.05$) was conducted in SPSS software to determine whether statistically significant differences existed between classes, and between datasets. Results indicated significant differences existed between classes ($F_{(2,625)}=22.924, p<0.001$) and between datasets ($F_{(1,625)}=6.041, p=0.014$). A pairwise comparison with Bonferroni adjustment indicated Class 3 was significantly different from the other two (all $p<0.001$) while Classes 1 and 2 were not significantly different from each other ($p=0.083$). Furthermore, the performance of the two datasets were found to be significantly different in Classes 2 and 3, but not in Class 1 ($p<0.001$).

Lessons learned
UAVs appear to be reasonable platforms for modelling the microtopography of treed bogs within western Canada, under most surface complexity conditions. However, estimated elevation errors increase with surface complexity, causing greater uncertainty within highly complex areas. Therefore, site conditions must be considered prior to adopting a UAV-based peatland mapping approach to determine whether anticipated elevation accuracies will be sufficient for the study purpose. The performance of LiDAR is not improved in areas of low complexity. However, elevations estimated by LiDAR data are greatly improved by UAV data in areas of moderate and high surface complexity. While overall elevation errors increase with surface complexity, incorporating supplemental UAV data somewhat offsets this effect. Therefore, in cases where highly accurate peatland elevation estimates are necessary, merging UAV and LiDAR data may be useful.

2.4. Estimating depth to groundwater table in a disturbed peatland using photogrammetric point clouds

Peatlands cover >30% of Alberta's boreal zone, store a large amount of soil carbon and exchange greenhouse gases (GHG) with the atmosphere. Fluctuation in depth to groundwater table at the plot level has been shown to strongly affect peatland Greenhouse Gas (GHG) emission (Harris and Bryant, 2009). Therefore, to estimate GHG emissions at the local and regional level across

different types of peatlands, it is necessary to accurately map the depth to groundwater table without the need to install numerous groundwater monitoring wells. Considering this scenario, the objective of this research is to develop an operational method to map groundwater table in a disturbed bog using UAV data and photogrammetric techniques. Our study area is located north of Peace River, AB within the Shell-Carmon Creek Lease (Figure 5). The site covers an area of ~700 m x 700 m, primarily representing an open to dispersedly treed bog.
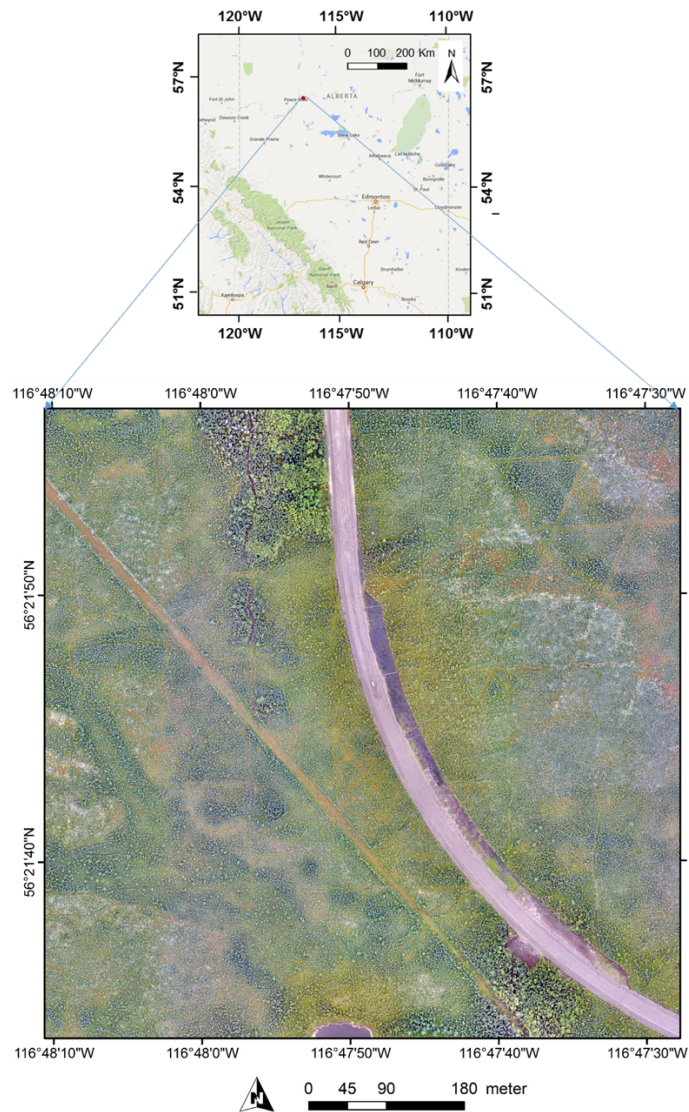
Figure 5: Location of the study area

Methods
We propose a new method that maps groundwater table by creating an interpolated surface of open water level (elevation) obtained from a UAV based orthophoto and photogrammetric point clouds. To do so, we first identified pockets of open water across the study area through classification, using RGB orthophotography and a canopy height model (extracted from photogrammetric point cloud) as inputs. We then extract point elevations from within these water bodies to create a sample

14

of visible ground water level (GWL). These samples are then interpolated to generate a full GWL surface. In order to transform GWL to depth to groundwater table (DTW), we subtracted the GWL surface from a detailed digital terrain model (DTM) that is, again, extracted from the photogrammetric point cloud.

Results and discussion

The microtopographic features (hummocks and hollows) that characterize natural peatlands are clearly visible, creating small variations in DTW (Figure 6). The impacts of the access road – high immediate DTW levels with inundated areas on the up-slope side – are readily apparent, as are the effects of small linear features (seismic lines and pipeline), which create low DTW values and ponding through the flattening of microtopography. The densely treed upland areas reveal generally high DTW values, in addition to interpolation noise caused by errors in the DTM.
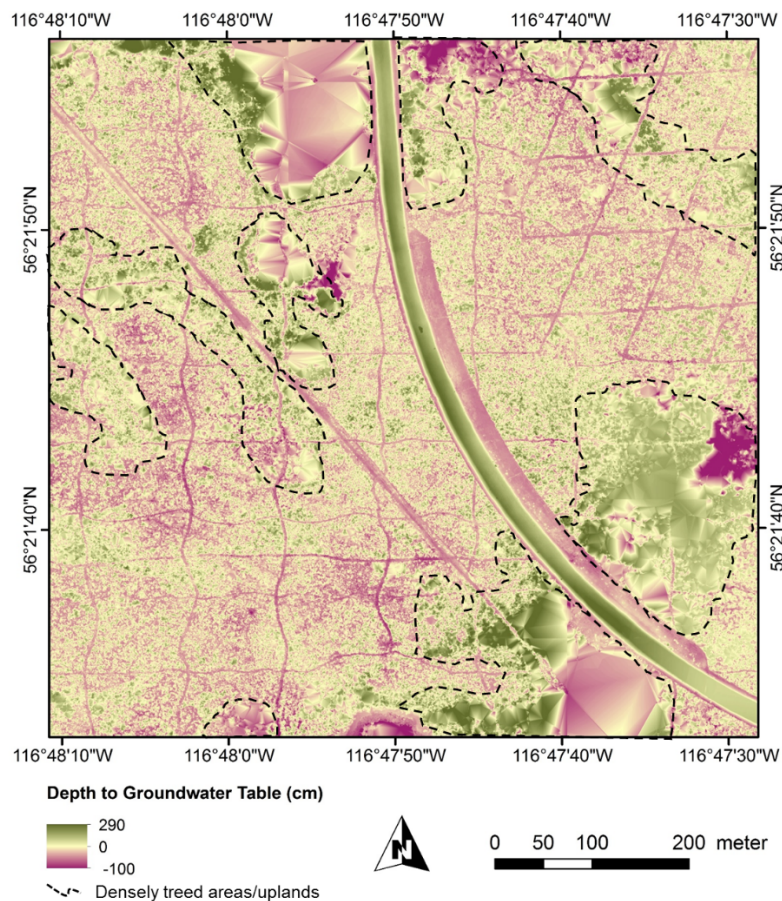
Figure 6: Predicted depth to groundwater table in the study area, where shades of green represent positive depth and shades of purple indicates negative depth (i.e., inundation).

<u>Lessons learned</u>
The major findings of this research include:
- Stable open water can be used to map groundwater table with acceptable accuracies.

- Compared to a undisturbed bog, seismic lines represent less micro topographic variability (hummocks and hollows) and lower overall depth to water table compared to its surroundings.

- Mineral roads across a wetland ecosystem (such as a bog) alter its hydrology.

- The accuracy of the model is influenced by the point cloud and the DTM generated from UAV data.

- As the surface complexity increases (partially to completely covered ground by canopy), it becomes increasingly difficult to see the ground and thereby to model the terrain and the groundwater table.

The proposed method offers a great potential option for deriving depth to groundwater table in disturbed and undisturbed peatlands and low-lying wetland areas, and thereby aids in estimating the GHG emissions from these ecosystems. Once successfully verified over different peatland types (bog, fen, swamp), our research will provide a pragmatic solution to reliably mapping depth to groundwater table using advanced remote sensing and photogrammetric techniques, which has numerous application across disciplines

2.5. Estimating the effects of low impact seismic lines on methane (CH_4) release in a forested boreal bog using UAV based remote sensing techniques

Peatlands are sensitive ecosystems, capable of releasing carbon to the atmosphere in the form of greenhouse gases (GHG) as a response to anthropogenic disturbances. Of particular concern is CH_4: a powerful GHG which has a reported 20-year global warming potential (GWP) that is 84 times greater than carbon dioxide (IPCC, 2014a; Zhu et al., 2014). The Intergovernmental Panel on Climate Change (IPCC, 2013) states that CH_4 emissions from natural wetlands are the primary driver of variability in global atmospheric CH_4 concentrations. However, the processes relating anthropogenic disturbances to CH_4 production and emission rates from wetlands are highly variable and poorly quantified, ultimately limiting our capacity to generate reliable global CH_4 estimates (IPCC, 2014b). Fortunately, local methane (CH_4) emissions are strongly linked to water table (WT) position and microtopography. Historically, these factors have been difficult to measure in the field, constraining our capacity to observe local patterns of variability. In this paper, we show how remote sensing surveys conducted from unmanned aerial vehicle (UAV) platforms can be used to map microtopography and WT over large areas with good accuracy, paving the way for spatially explicit estimates of CH_4 emissions.

The objective of this research is twofold: first, to compare two methods of estimating CH_4 release from a treed-bog study site in northern Alberta, Canada: (i) microtopography and (ii) DTW, both derived from UAV data; and second, to quantify the impact of LIS lines on CH_4 release, microtopography, and WT across our study site. The study site is ~61 ha portion of a treed-bog located roughly 35 km northeast of Peace River, Alberta. Within this larger study site, a 3.8 ha

subset area was used to assess model accuracies and generate CH_4 estimates for up scaling across the full site.

Methods

CH_4 samples and depth to groundwater table (WT) were collected at 27 field sampling points (collars) every second week over a 150-day monitoring period to develop an empirical relation between CH_4 and microtopography/WT. Flux- sampling points were identified as either hummocks or hollows based on vegetation and microtopographic characteristics. From this segregation, the average CH_4 flux per microform (hummock vs. hollow) was calculated. We then determined the relationship between CH_4 emission and DTW by applying a LOG10 transformation to the 150-day mean CH_4 flux data of each plot, and performing a linear regression with WT position of each corresponding water well.

UAV data were also acquired to create mictotopography (MT) and WT surface of the study area. Microtopography surface (terrain) was generated using the method developed by Lovitt et al. (2017) and WT surface was generated using the method developed by Rahman et al. (2017). Microtopography surface is further classified to hummocks and hollows. The empirical relation developed between CH_4 and microtopography/WT using field data was used in the UAV based microtopography and WT surfaces to estimate CH_4 emissions for the study area subset. Additionally, the difference between estimated CH_4 flux in undisturbed and disturbed (seismic lines) areas was calculated to determine the impact of seismic lines on CH_4 release.

Results and discussion

Table 9 summarizes partial (undisturbed vs disturbed) and total (undisturbed + disturbed) CH_4 flux estimates for the study site as calculated by both surfaces, as well as estimated increase (%) of CH_4 along seismic lines. Significant differences were noted between the two surfaces when predicting CH_4 flux in undisturbed areas ($p<0.01$) but not along seismic lines ($p=0.454$). Total CH_4 for the 3.8 ha study site over the 150 day flux monitoring period was estimated as 124 kg using MT and 76 kg using DTW, resulting in the MT surface estimating 48 kg CH_4 more than the DTW. CH_4 emissions are predicted to increase substantially (MT: +20%, DTW: +120%) on seismic lines relative to undisturbed peatland. Results of the statistical analysis indicate these differences are significant ($p<0.01$) in both surfaces (MT & DTW).

Table 10 represents estimates of CH_4 flux across the entire 61 ha treed-bog site. Excluding other disturbance features like pipeline and road, LIS account for approximately 5.2% total site coverage. Assuming the site had 0% seismic line disturbance, total site CH_4 emission (standard error) estimated over the 150-day monitoring period is predicted to be between 1,130 kgCH_4 (30) (DTW) and 1,990 kg CH_4 (13) (MT). Adjusting these predictions to include 5.2% LIS disturbance, total CH_4 emission estimates increase to 1,200 kg CH_4 (15) (DTW) and 2,010 kg CH_4 (2) (MT) respectively. This translates to an increase in CH_4 emissions at the 61 ha site over the 150-day monitoring period of approximately 70 kg and 20 kg, respectively.

Table 9: Predicted CH_4 emissions (standard error) of 3.8 ha subset study site over 150-day monitoring period and estimated increase (per ha) due to seismic line disturbance

		MT surface	DTW surface
Undisturbed	Total estimated CH_4 flux (kgd^{-1})	0.759 (0.0003)	0.433 (0.0006)
	Total area (ha)	3.78	3.78
	Avg predicted flux (kgha^{-1}d^{-1})	0.216 (0.1)	0.123 (0.3)
Disturbed	Total estimated CH_4 flux (kgd^{-1})	0.070 (0.0003)	0.072 (0.0004)
	Total area (ha)	0.269	0.267
	Avg predicted flux (kgha^{-1}d^{-1})	0.261 (0.3)	0.270 (3.0)
Total Site	CH_4 increase per ha due to disturbance	20%	120%
	Percent of site disturbed	7%	7%
	Total predicted flux for site (kg$\cdot$3.8 ha$^{-1}\cdot$150 d^{-1})	124	76

Table 10: Estimated total CH_4 emission across 61 ha study site and predicted increase over 150-day monitoring period due to seismic line disturbance

	Undisturbed	**Disturbed**
Areal coverage	94.8%	5.2%
MT flux (kgha^{-1}d^{-1})	0.216	0.261
DTW flux (kgha^{-1}d^{-1})	0.123	0.270

	MT surface	DTW surface
Total predicted flux in undisturbed areas (kg$\cdot$ha$^{-1}\cdot$d^{-1})	1.25	0.71
Total predicted flux in disturbed areas (kg$\cdot$ha$^{-1}\cdot$d^{-1})	0.08	0.09
Theoretical total predicted flux of site (disturbance = 0%) (kg$\cdot$ha$^{-1}\cdot$d^{-1})	1.32	0.75
Actual total predicted flux of site (disturbance = 5.2%) (kg$\cdot$ha$^{-1}\cdot$d^{-1})	1.33	0.80
Absolute total site CH_4 increase due to disturbance (kg $\cdot$61ha$^{-1}\cdot$150d^{-1})	20	70

Flux reported in units: kg per site area in ha per day (kg$\cdot$ha^{-1}d^{-1})
Flux reported in units: kg per site area in ha per 150 days (kg $\cdot$61ha$^{-1}\cdot$150d^{-1})

This research represents an initial attempt to determine how LIS have altered boreal peatland carbon balance and storage functions at a single forested bog in northern Alberta. However, peatlands are incredibly diverse ecosystems and we encourage additional studies building upon our methods, and/or aimed at investigating similar disturbance features within different peatland types.

Lessons learned

We determined that seismic lines have significant impacts on the peatland ecosystem, causing overall flattening of microtopography and decreasing DTW, resulting in significant increases in CH_4 release. Based on our assessment, and the knowledge that seismic lines are widespread within the western Canadian Boreal region, we suggest these linear disturbances should be included in land use change GHG emission estimation to avoid under reporting at the national scale. Furthermore, due to the noted degree of microtopographic and DTW disturbance, we posit that active restoration will likely be necessary to achieve recovery of vegetation and ecosystem function along seismic lines. Additional data are required to properly validate the CH_4 flux estimates and determine which UAV method is superior; however, we believe the relationships presented here (significant increase in CH_4 emission along seismic lines) are valid based upon the assessment of altered physical parameters (microtopography and DTW).

2.6. Potential impact of seismic lines on peatlands in Alberta to methane emissions

Peatlands cover 16% of Alberta's land area, representing an important soil C stock. Anthropogenic disturbance, such as oil sands exploration and extraction, can alter peatland C cycling (e.g., Rooney et al., 2010), but the effects have not been quantified for many disturbance types. Seismic lines are constructed for geophysical mapping of oil reserves. Until the early 1990s, these lines were often cleared by bulldozers, creating 5-10 m wide linear features. Since then, these 'legacy' lines have been replaced by 'low-impact' seismic (LIS) lines in Alberta and elsewhere in Canada (e.g., British Columbia, Yukon, Northwest Territories), with a reduced width (1.5-5 m) and slightly meandering path designed to reduce ecological impact (Dabros et al., 2018). Seismic lines are the most abundant anthropogenic disturbance in the boreal forest (Pasher et al., 2013) and likely increase CH_4 emissions from peatlands (Lovitt et al., 2018); however, the extent of this impact at a provincial scale has yet to be quantified. The objectives of this project were to: 1) estimate the total area of peatland impacted by seismic lines in Alberta and 2) estimate CH_4 emissions induced by these disturbances.

Methods

The seismic line data (GIS Layer) was obtained from Alberta Biodiversity Monitoring Institute's (ABMI) Wall-to-Wall Human Footprint Inventory database (ABMI, 2017) that depicts anthropogenic disturbances across the province in 2014. ABMI is entitled to collect, update (every two years) and distribute data on human footprint across the province of Alberta, Canada under the Alberta Human Footprint Monitoring Program (AHFMP). The Alberta Merged Wetland Inventory (polygon features; Alberta Environment and Parks, 2017) and the provincial seismic lines (line features) were intersected to identify seismic lines that fall within wetland. Linear length of different types of seismic line falling in different class of peatland (we included bogs, fens and swamps as peatlands for this study) was then calculated from this intersected layer. In the next step, the lines were converted to polygons by buffering around the line to obtain corresponding

line widths. This polygon layer was used to calculate the area of different types of seismic lines within different types of peatlands.

We compiled literature values for methane (CH_4) flux from study sites in boreal continental western Canada (Manitoba, Saskatchewan, Alberta, Northwest Territories; Vitt et al., 2000) for bogs and fens. Although our case study focused on Alberta, we included data from a broader geographic region due to the scarcity of peatland CH_4 flux measurements in Alberta. As we could find very few records of CH_4 flux for swamps in western Canada, all Canadian sites for swamps were used. When data from multiple sample plots were present in the data set, we took each plot as an individual data point if WT was also measured at each plot. As our goal was to develop a CH_4 flux-WT regression equation, we chose to maintain this plot-based data as it represents the scale at which WT and CH_4 vary spatially in peatlands. We used the mean CH_4 and WT during the measurement period, which included only the warm season (usually May – August/September). For each peatland class (i.e., bog, fen, swamp) we created a separate regression equation with $\log_{10}(CH_4 + 2)$ flux of the mean daily values as the dependent variable and mean WT position of the same measurement period as the independent variable in R (R Core Team, 2016). The log transformed data was used to improve normality and homogeneity of the residuals of the regression. Based on our compiled data set, we estimated the mean summer WT position for each peatland class. Using this WT position and the regression equation, we estimated the mean CH_4 flux for each class. We converted this value to an estimate of annual CH_4 emissions assuming a 123-day emission period (May-August).

Next, we moved the mean WT position closer to the surface of the peatland by 13.9 cm and 15.4 cm based on measured hydrologic impact of seismic lines on peatlands in Alberta (Strack et al., 2018; Lovitt et al., 2018). We then recalculated the new CH_4 emission from the area of seismic lines occurring on each peatland class and estimated a new annual peatland CH_4 emission for the province. The difference between this estimate and the original estimate based only on mean WT is reported as the potential effect of seismic lines on peatland CH_4 flux.

Results and discussion
Based on the data sets used, we estimate that at least 345,000 km of seismic lines (including trails which can be industrial or recreational and can be generated from abandoned linear features such as roads or old fire guards as well as detours from seismic lines) cross peatlands in Alberta, of which about 10% are LIS lines (Table 11). Considering average widths of each disturbance type, the area of peatland disturbed by seismic lines and trails in Alberta is over 1900 km^2. We expect these figures to be lower than the true amount of disturbance. While the ABMI Human Footprint Inventory data is the best source of publically available information, its mapping protocol relies extensively on satellite imagery that likely misses many small disturbances such as LIS. Using a case study area of 10,000 km^2 in central Alberta, we determined that the ABMI Human Footprint Inventory captured only 53% of the seismic lines and trails.

Regression equations between log-transformed CH_4 flux and water table (WT) position were statistically significant ($p < 0.05$) for each peatland type. Based on our compiled database of peatland CH_4 flux and water table (WT), we determined a mean WT position of -18 cm, -8 cm and -21 cm for undisturbed swamps, fens and bogs, respectively (where negative values indicate distance below the ground surface) leading to estimated mean emissions of 1.4, 7.1 and 2.5 g CH_4

m^{-2} yr^{-1}. These values are on the low end of ranges of CH$_4$ fluxes reported in recent compilations of northern peatland data (Abdalla et al., 2016; Turetsky et al., 2015) – not surprising given the dry continental climate in western Canada. Using these mean values, we estimated province-wide CH$_4$ emissions from peatlands as 0.25 Tg (95% confidence interval: 0 – 3.2 Tg) without any disturbance. Considering wetter conditions on the seismic lines and the area impacted in each peatland type, we estimate that seismic lines increase peatland CH$_4$ emissions in Alberta by 4.4 to 5.1 kt CH$_4$ yr^{-1} (Table 11). Using a global-warming potential for CH$_4$ of 28 CO$_2$-e over a 100-year time frame[31], this increase in CH$_4$ emission is equivalent to 0.12 to 0.14 Mt CO$_2$-e yr^{-1}.

The Paris Agreement highlighted the importance of accelerating the reduction of global anthropogenic GHG emissions and recognized the importance of conserving and enhancing sinks and reservoirs of GHGs as appropriate (UNFCCC, 2015). Therefore, there is an urgent need to better quantify the effect of seismic exploration on peatland carbon and greenhouse gas exchange. We recommend employing a multi-scale approach aimed at determining local factors driving changes in carbon uptake and CH$_4$ emissions, combined with improved mapping of shifts in ecohydrological conditions over regional scales.

Table 11: Summary of peatland and seismic line area and impact on methane emission

Peatland type	Bog	Fen	Swamp	Total[a]
Total area in Alberta (km^2)	30050	58580	46160	**134790**
Total length of seismic lines[b] (km)	88580	144580	112480	**345640**
Total area[c] covered by seismic lines (km^2)	490	790	630	**1910**
Average CH$_4$ undisturbed (g CH$_4$ m^{-2})[d]	1.1	3.4	0.40	
CH$_4$ flux on seismic line (g CH$_4$ m^{-2})[d]	2.5 - 2.8	7.8 - 8.5	0.80 – 0.85	
Enhanced CH$_4$ flux due to seismic lines (t CH$_4$)	690-800	3440 – 4010	250 – 290	**4430 – 5140**
(kt CO$_2$-e)	19 – 22	97-113	7 – 8	**124 – 144**

a. Values may not add to total due to rounding
b. Total of conventional, low-impact seismic lines and trails.
c. Estimated based on average widths of each line type as given in the ABMI database
d. Estimated from mean daily fluxes during summer extended over 123 day growing season. Winter fluxes assumed negligible. See Methods for more information.

With LIS comprising much of the on-going disturbance, accurate estimation will likely require increased access to industrial disturbance records: an issue mediated by provincial governments in Canada. Moreover, improved mapping of swamps and studies to characterize carbon exchange and impact of disturbance on this wetland type is needed to reduce uncertainty related to peatland seismic line impacts. Efforts on these fronts will enable the development of emission factors and activity data to improve the accuracy and completeness of national reporting of anthropogenic GHG emission estimates related to land use, as well as provide the process-based understanding needed to mitigate these emissions.

Lessons learned
Seismic lines result in the greatest area of anthropogenic disturbance in boreal Alberta. We estimate that at least 1900 km^2 of peatland have been impacted. Total area impacted in very likely underestimated given the underrepresentation of LIS lines in provincial databases. Potential increases in CH_4 emissions related to this impact were 4.4-5.1 kt CH_4 yr^{-1}, although this is likely conservative. Including this in national reporting of land-use impacts on GHG emissions would increase the current estimate by 7-8%. Direct measurements of GHG exchange on peatlands impacted by seismic lines is needed to better understand their impact at local and landscape scales.

2.7. Land cover alteration by peatland road crossings

Peatland ecosystems are an important land cover type in boreal regions, covering an average of 30% of the region in Canada. Increasing resource exploration and extraction has resulted in the construction of an extensive road network across Canada's boreal forest, such that linear disturbances now account for the greatest area of disturbance in the region. The construction of roads crossing peatlands disturb the area directly under the road footprint, but may also alter conditions in the adjacent areas. The objective of the study is to determine road-induced land cover change (type and extent) in two peatland sites with unpaved resource roads using World View 2 and Geo Eye 1 imagery by comparing land cover before and after road construction. Our study took place in the Boreal Forest natural region of northwestern Alberta, Canada. We worked in two (~1 km x 1 km) areas of interest that are located to the north of Peace River, AB, Canada, within the Carmon Creek watershed (Figure 7). One of the sites is characterized as a forested bog and the other as shrubby rich fen.

Methods
We investigate the changes in land covers due to the construction of a mineral road in two peatland sites in Northern Alberta. To do so, we obtain multispectral satellite data (World View 2 and Geo Eye 1) and 3D structural information (from LiDAR and UAV based photogrammetric point cloud) ~3 years before and ~ 3 years after the construction of the roads. We then separately classify the before images and the after images into representative land cover classes. The classified images are then compared to locate and quantify land cover change due to the construction of road.
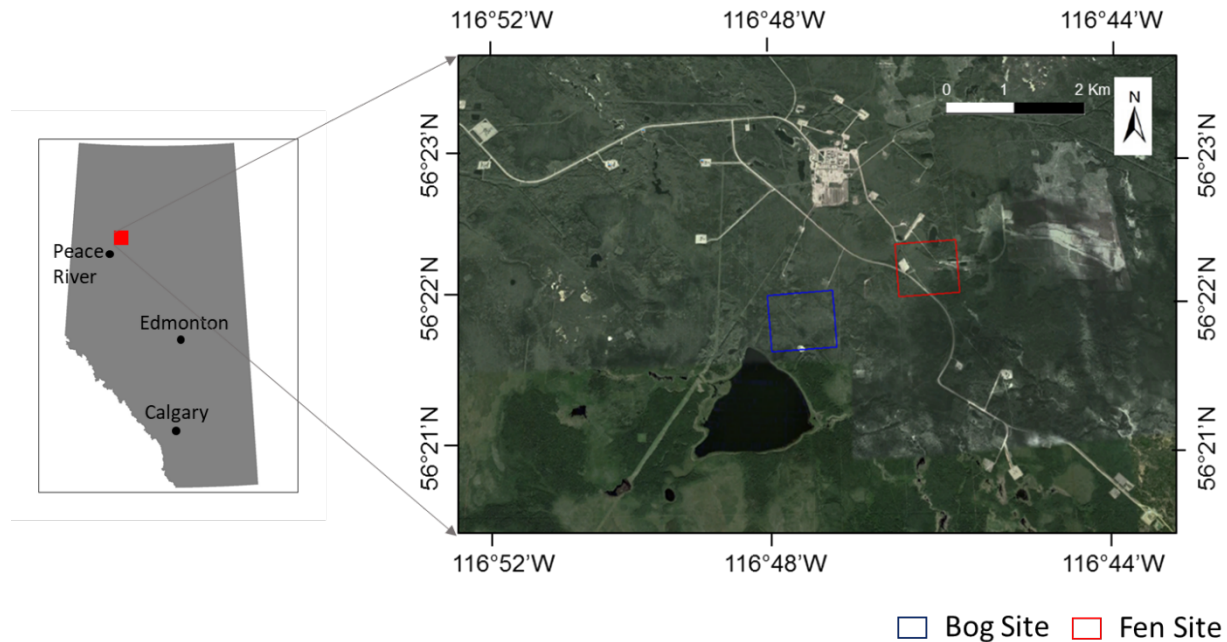
Figure 7: Location of the study area

Results and discussion
Figure 8 represents a change map of the Bog Site where the land cover change areas are highlighted using different colors and the arears that are not changed are colored light grey. It is fair to say that most disturbances occur by the side of the road and it extends to ~40 m from the edge of the road. The statistics presented in figure (Figure 9) also support this statement. However, the impact is more on the upstream side (East) of the road, where the ground is observed to be flooded and forest/undisturbed ground is degraded.

Figure 10 represents a change map of the Fen site where the land cover change areas are highlighted using different color and arears that are not changed are colored light grey. Like the bog site, most disturbances occur by the side of the road and it extends to ~30-40 m from the edge of the road. The statistics presented in Figure 11 also support this statement. However, unlike the bog site impacts are more or less evenly distributed on both sites of the road. This might be because the general direction of the water flow is more or less along the road at this site. A hotspot of disturbance is observed to the north side of the road at the eastern corner. This might be due to construction of another access road in that area.

Lessons learned
The major findings of this research include:
- Construction of mineral road in peatland alters surrounding land cover.

- The impact is highest by the side of the road and gradually decreases as the distance from the road increases. The impact is observed to extend to ~40 m away from the road.

- Placement of a mineral road across the general direction of groundwater flow causes flooding on the upstream side and drying on the downstream side. However, when the road is constructed roughly along the flow direction, the disturbance is observed to be evenly

distributed on both sides of the road. From this, we can also estimate that the impact on local hydrology is maximum when the road is perpendicular to the general direction of groundwater flow. In contrary, the impact is minimum when the road is parallel to the general direction of groundwater flow.
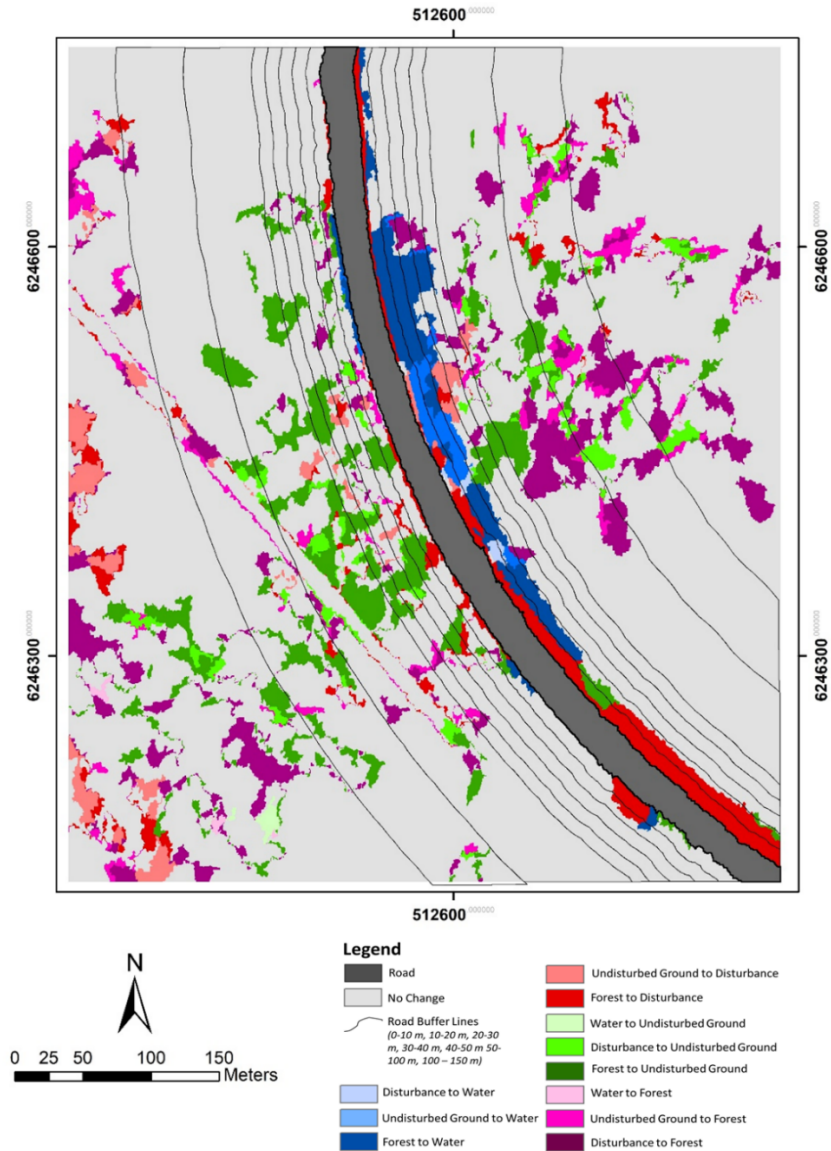
Figure 8: Change map for the bog
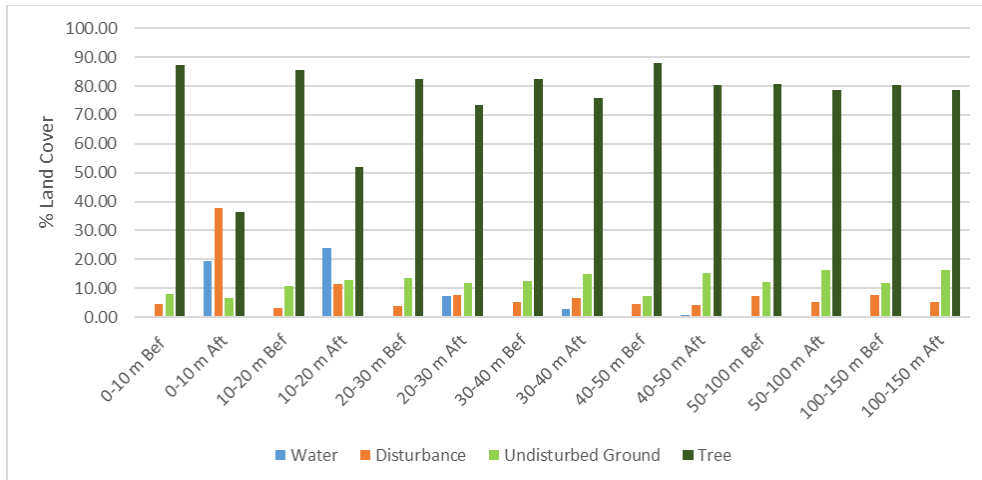
Figure 9: Change in land covers after the construction of the road in the Bog site. The changes are stratified by distance from the road.
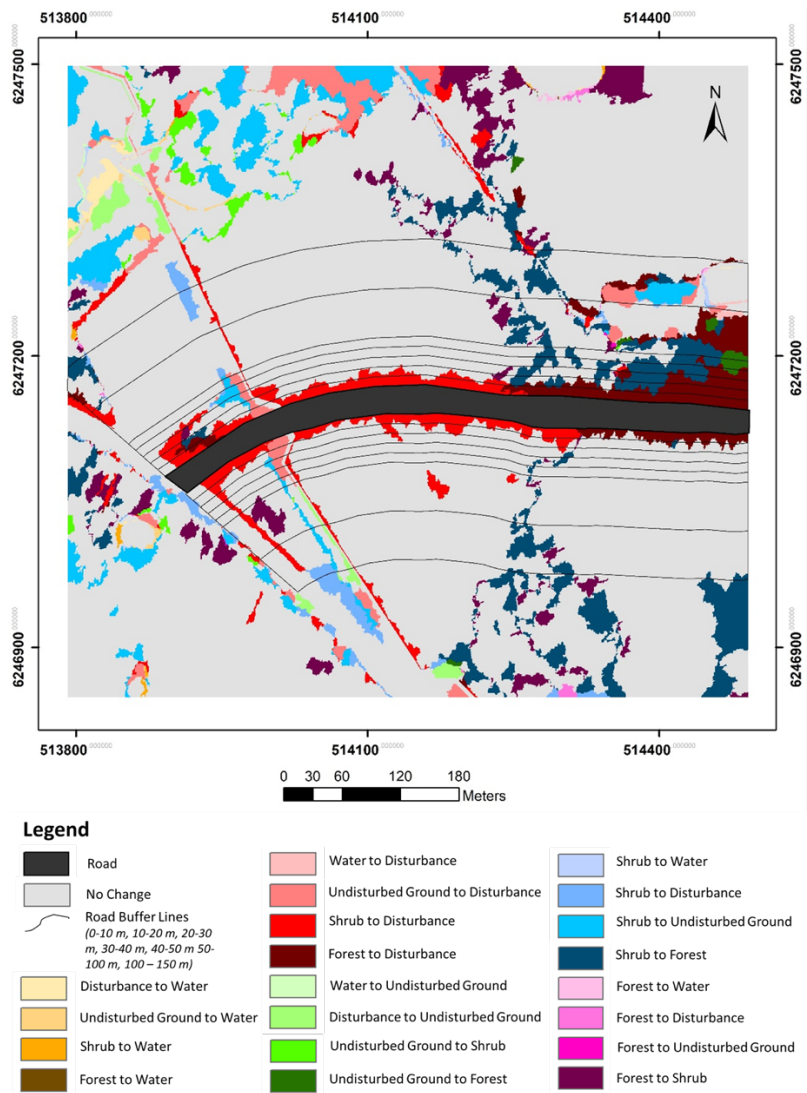
Figure 10: Change map for the fen
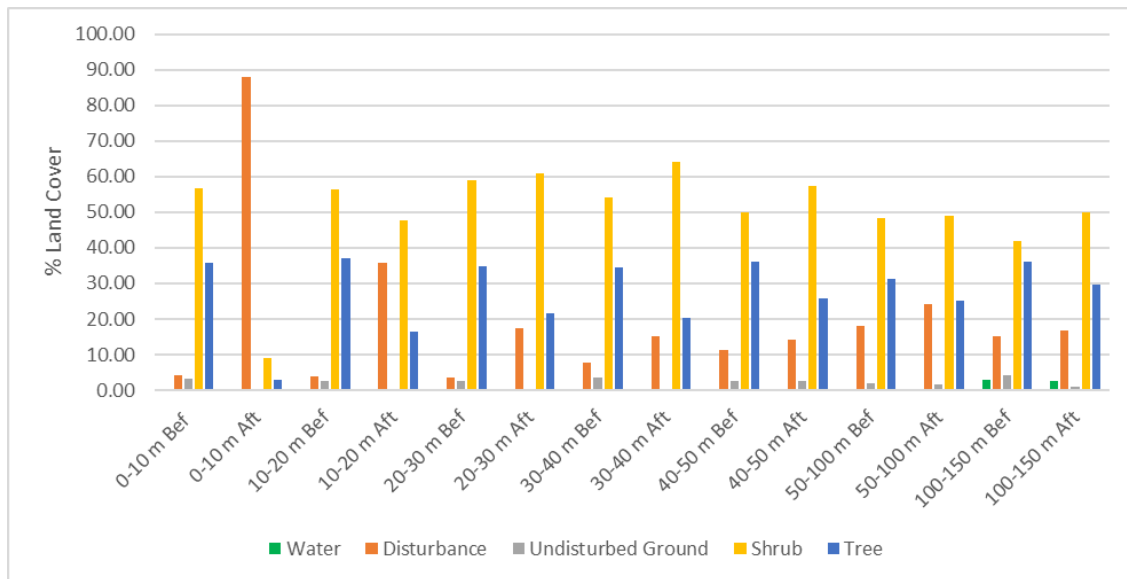
Figure 11: Change in land covers after the construction of the road in the Fen site. The changes are stratified by distance from the road.

2.8. Impact of resource access roads on hydrological conditions of boreal forested peatlands

Resource road construction through boreal peatlands has the potential to modify peatland ecosystems and peat accumulating function as the road construction involves vegetation clearance, logs and/or geotextile laying, and mineral soil deposition (Graf 2009). The road fragments a peatland into two parts i.e. upstream and downstream. As a result of the fragmentation, the two fragments can be disconnected from the surface and subsurface water flow or connections and it is expected to observe a higher water table with respect to the surface (DTW) on the upstream, and lower DTW on the downstream part of the fragmented peatland (Gillies 2011; Partington and Clayton 2012; Badiou and Page 2014; Plach et al 2017). Moreover, since resource roads are constructed using mineral fill, the compression level of a road will reduce the hydraulic conductivity beneath the road, but increase the surface flow, which increases mineral soil and nutrient deposition into fragmented peatland area connected to the road. It is also possible that the edges of the road become subsided and mixed into the upper layer of peat, creating the potential to alter the whole ecosystem along the road. The altered ecosystem may show different hydrological properties. However, the level of impact largely depends on the distance from the road, the streams of the fragmented parts, and the position and laying of culverts. Therefore, the objective of the study was to quantify the impact of resource access roads on hydrological properties of boreal forested peatlands.

Methods

To measure the hydrological properties (e.g., DTW, hydraulic conductivity (K_{sat}), hydraulic heads (HHs)) of the study area, a set of six perpendicular transects were established in both bog and fen in 2015. In each transect, six wells (PVC pipes, 1 m deep and 3 cm in diameter) were installed. In

26

addition, three wells were installed at 50 m (references areas) away from the road in both bog and fen (total 78 wells). Those water wells were installed at an interval of 2, 6 and 20 m on both sides of the road in both sites.

Transects associated with culverts were named as low impact (LI) transects (n=6) distributed equally in both bog and fen. Whereas, high impact (HI) transects (n=6) were established at least > 20 m away from culverts. Moreover, a total of 14 nests of piezometers with each nest consisting of three depths (i.e. 50, 100 and 125 cm deep in the bog site and 25, 50 and 100 cm deep in fen) were installed along a HI and a LI transect (at 2, 6 and 20 m distance) and undisturbed areas. DTW was recorded bi-weekly (May to September 2016, and May to August 2017) with the help of a blow-pipe. In addition, K_{sat}) and HHs were recorded.

Results and discussion

In terms of topography, a gradual decrease from the upstream (east) to downstream (west) areas in the surface elevation was observed in bog with the slope more clearly perpendicular to the road on the northern end of the study site. Whereas, no significant pattern was observed in fen - slope in the upland on the south side nearly parallel to the road. This suggests that the surface water in the bog has been blocked compared to the fen.

We found that the mean bog (-11.29 cm) and fen (-2.51 cm) DTW positions in 2016 were significantly shallower compared to the mean DTW positions of bog (-19.16 cm, z =7.58, p < 0.001) and fen (-17.91 cm, z =13.14, p < 0.001) in 2017. Thus, DTW position in fen was significantly shallower compared to bog in 2016 (z = 12.04, p < 0.001), but not in 2017 (z = 0.91, p = 0.364).
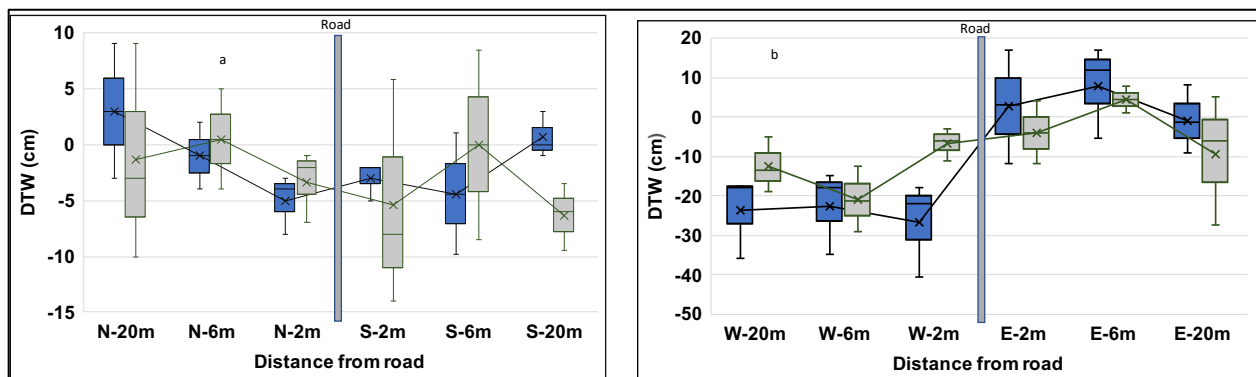
Figure 12: Impact of access road on depth to water table (DTW) in the: a) fen, where blue box plots represent HI transects (> 20 m away from the culverts) and grey box plots represent LI transects (< 2 m away from the culverts); and b) bog, where blue box plots represent HI transects (> 20 m away from the culverts) and grey box plots represent LI transects (< 2 m away from the culverts) in 2016.

Bi-weekly DTW observations (Figure 12) showed bog average DTW positions at ≤ 20 m (-11.0 ±1 .6 cm) and 50 m (-16.4 ± 1.7 cm) away from the road were significantly shallower than areas

> 150 m from the road in 2016 (z = 2.86, p < 0.01; z = 3.27, p < 0.001), respectively. In contrast, fen average DTW position at ≤ 20 (-2.6 ± 1.5 cm) and 50 m (-2.6 ± 0.7 cm) from the road in 2016 were not significantly different than areas located > 150 m from the road (z = 0.09, p = 0.925).

At sites within 20 m distance from the road, in the bog, all interactions of the factors (side of the road, distance from the road, and the culvert position) were significant on DTW position in both 2016 (F $_{(2,449)}$ = 11.08, p < 0.0001) and 2017 (F $_{(2,375)}$ =7.90, p < 0.001; Table 1, Fig. 3). In general, the Tukey's HSD test showed that the average DTW positions on the upstream areas, independent of distance from the culvert, were significantly shallower than the downstream areas in both 2016 and 2017 (p < 0.001) in the bog.

Within upstream areas, the 2 and 6 m plots were wetter than the 20 m plots in both HI and LI transects. The shallowest and deepest DTW positions were observed at the HI upstream 2 m and HI downstream 2 m areas, respectively. Post – hoc comparisons also revealed that the DTW at LI downstream 2 m plots was significantly shallower compared to 6 and 20 m plots at LI downstream areas and all plots of HI downstream areas. Also, the recorded peat moisture content was ~ 90% in all areas irrespective of DTW position. However, in fen, there was no significant effect on DTW based on the culvert position, side of the road and distance from the road.

Table 12: Mean water table depth (DTW) ± standard error (SE) in the bog and fen, Carmon Creek, Peace River, Alberta.

Sides of the road	Year	Mean DTW ± SE (cm)	
	2016	**Bog**	**Fen**
Upstream		-1.1±1.6	-1.5±1.0
Downstream		-20.8±1.5	-3.6±1.2
	2017		
Upstream		-10.6±2.3	-14.6±3.6
Downstream		-25.5±2.3	-14.5±4.4

Also, the effect of culverts on DTW immediately adjacent to the road, based on the GWL recorded from the wells adjacent to roads, showed a significantly shallower DTW (-7.5 cm; p < 0.001) on the upstream areas of the road compared to the downstream areas (GWL = -27.1 cm), but the difference declined closer to the culvert. Also, lateral GWL positions in the bog showed a lower difference between upstream and downstream DTW positions up to ~ 15 m along the road edge from a culvert (Figure 13). This suggests that culverts help to connect fragmented part of the peatlands. In contrast, we did not see a significant pattern of the DTW variation in measurements moving away from the culvert in the fen site.
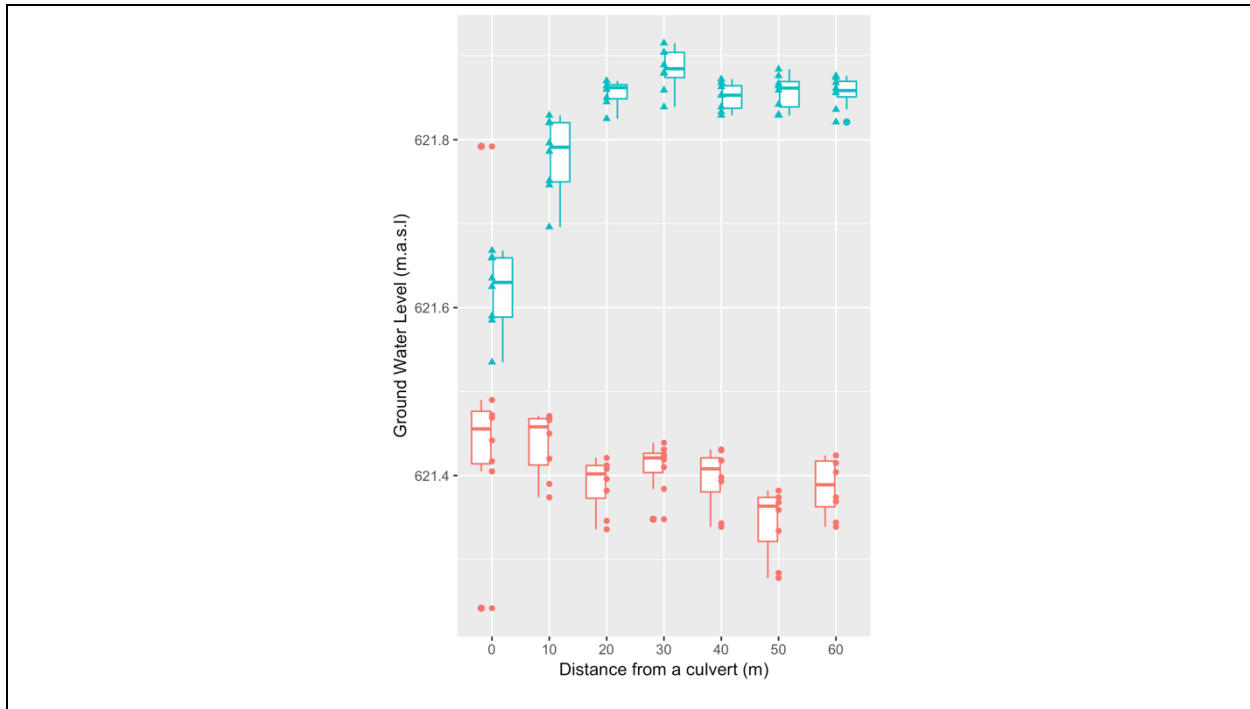
Figure 13: Mean GWL position of water wells located parallel to the road at an interval of 10 m from a culvert in the bog. Red box-plots represent downstream areas of the road and blue represent upstream areas of the road.

Lessons learned:
Installations of culverts help to connect the fragmented parts of peatlands. However, it is important to consider the water flow- direction, distance between culverts, and types of the peatland before installing culverts. Results from the bog suggest that culverts should be separated by less than 20 m to reduce hydrologic impacts when the road crosses perpendicular to the slope of the peatland.

2.9. The impact of resource access roads on boreal forested peatland enzymatic activities

The construction of resource access roads across boreal peatlands has become a common practice in Canada. As shown in section 2.8, these access roads have a potential to interrupt the natural flow of water across fragmented parts of the peatland resulting into a new water table regime (e.g. ponding on the upstream and drying up of the downstream part of the peatland). Accordingly, the pattern of anoxic conditions changes, which lead to the acceleration of oxygen diffusion in drier areas and hence may stimulate the enzymatic activities (hydrolase and phenol oxidase activities) that are linked to the higher rate of decomposition and increased CO_2 from peatlands (Freeman et al., 2001). However, there is no published research investigating the impact of access roads on enzymatic activities in boreal peatlands. Therefore, this study was conducted to document and analyze the impact of the road on enzymatic activities.

The objective of the study was to determine the impact of access roads on the enzymatic activities of boreal forested peatlands.

Methods
The study was conducted in a boreal forested bog and a shrubby rich fen in Carmon Creek, Peace River, Alberta. In 2015, a set of six perpendicular transects were established in each site (bog and fen) equally distributed in areas along the culverts (< 2 m) and > 20 m from culverts. A total of 39 peat samples of approximately 5 cm x 5 cm from the surface were collected (six-peat samples from each transect at 2 m, 6 m, and 20 m from both sides of the road and three samples from natural areas) from both bog and fen. In addition to peat sampling, water table depth (WT) was also recorded from the corresponding wells (Polyvinyl chloride, 1 m deep and 3 cm diameter) installed beside each sampling plot. Collected peat samples were stored at -20 °C to prevent the enzymatic decomposition of peat (Lee et al., 2007) and transported to the University of Waterloo for the laboratory analyses. All samples were assayed for phenol oxidase and hydrolase enzymes by following the method of Dunn et al., (2014). The obtained dry weight was used to calculate the carbon content and soil organic matter percentage (SOM%), which were used to measure the enzymatic activities (Saraswati et al., 2016). Moreover, phenolic concentrations were also measured with Folin-Ciocalteu phenol reagent by following the method of Box (1983).

Results and discussion
There was ~ four times higher average hydrolase activity in the fen (16.88 nmol g^{-1} min^{-1}) compared to the bog (t = 5.84, p < 0.001). Specifically, average activities of glucosidase, sulfatase, glucosaminidase and phosphatase were all significantly higher in the fen (t = 4.99, p < 0.001; t = 3.65, p < 0.001; t = 4.24, p < 0.001; t = 2.41, p = 0.01) compared to the bog. However, average phenol oxidase activity in the bog (0.24 μmol g^{-1} min^{-1}) and fen were similar (0.17 μmol g^{-1} min^{-1}; t = 0.90, p = 0.36).

We found significant effects of culvert distance, side of the road, and distance from the road on enzyme activities with highest activity close to the road on the downstream side far away from culverts. Significantly higher phenol oxidase activity was observed on the downstream side of the road far from culverts (t = 3.02, p = 0.03) and upstream side connected by culverts (t = 3.161, p = 0.02). Also, phenol oxidase activity was significantly higher on the downstream side compared to the upstream side and at 6 m distance from the road.

This could be due to water ponding on the upstream side of the road at the bog likely decreased oxygen availability and resulted in lower phenol oxidase activities, which ultimately helped to increase the concentration of phenolics in the upstream areas. In contrast, on the downstream side, particularly in areas not directly connected by culverts, the lower WT position relative to the peat surface would have enhanced the diffusion of oxygen into the deeper layers of peat. This may have helped to trigger phenol oxidase activity, resulting in greater decomposition of organic matter, as reported elsewhere (Freeman et al 2001; Kang et al 2005). This mechanism for the increased decomposition of organic matter is supported by the negative correlations between both WT position and the concentration of phenolics with phenol oxidase activity in the bog. However, no significant impact of the road was observed in the fen in terms of enzymatic activities. Details can be found in Saraswati et al. (2019).

We found that an access road had significant impacts on enzyme activities in a forested bog, where the road was perpendicular to water flow, but not in a fen, where the water flow was largely parallel to the road. We observed significantly higher phenol oxidase and hydrolase activities in the road disturbed areas compared to undisturbed areas of the peatlands. This indicates that peatland road crossings alter carbon and nutrient cycling.

2.10 Greenhouse gas emissions induced by access road crossing in boreal forested peatlands and the mitigation potential of culverts

The boreal and subarctic regions have approximately 95% of the total peatlands in Canada (Tarnocai et al., 2011) and they store a significant amount of carbon (~550 Gt of organic carbon) in their peat (Yu et al., 2010). The various factors responsible for storing such a tremendous amount of carbon in the form of peat are low pH, anoxic conditions, deep layers of water saturated peat, low enzymatic activities, and low nutrient availability in peatlands. At the same time, these peatlands are sources of methane (CH_4), which is another important greenhouse gas (GHG; Abdalla et al., 2016; Saunois et al., 2016) having ~ 28 times the global warming potential of carbon dioxide (CO_2) over a 100 year period (Myhre et al., 2013).

However, these peatlands have been facing various human-induced disturbances including natural resource (e.g. petroleum and forestry) exploration and extraction. These practices require the construction of resource access roads (Partington and Clayton 2012) across peatlands. These roads fragment peatlands and may bring various complex feedbacks to the peat accumulation rate by impacting the peatland's primary productivity and decomposition function due to altered hydrological, biological, physical, and chemical properties of peatlands. Ultimately, the altered peatland ecosystem areas can have a varying level of GHG emission scenarios. The impacts may differ among peatland types and can vary both spatially and temporally.

The objectives of the study were:
1. To determine the impact of the road on carbon (CO_2) fluxes (NEE and NPP) from boreal peatlands.
2. To study the impact of the road on methane (CH_4) and nitrous oxide (N_2O) emissions from boreal peatlands.
3. To evaluate the reduction in induced emissions by culverts

Methods
A set of six perpendicular transects were laid in both (bog and fen) study sites. In each transect, six metal collars (60 x 60 cm) have been installed to a depth of 10 -15 cm in the peat for GHG flux sampling. Collars were installed at the interval of 2 m, 6 m and 20 m on both sides of the road (total 39 collars in each study site). Besides each collar, corresponding wells (PVC pipes; 1 m deep and 3 cm diameter) were also installed. Transects associated with culverts were named as low impact (LI) transects (n=6) distributed equally in both bog and fen. Whereas, high impact (HI) transects (n=6) were established at least 20 m away from the culverts.

Closed chamber method was employed to measure GHG (CO_2, CH_4 and N_2O) fluxes every second week from each collar (May to September 2016 and May to August 2017). Gas samples (for CH_4 and N_2O) were collected from each collar by fitting a closed opaque chamber (60cm x 60 cm x 30 cm) at the interval of 7, 15, 25 and 35 min. Samples were stored in pre-evacuated Exetainers. The collected samples were analyzed by a Shimadzu GC-2014 gas chromatograph at Waterloo University.

The dynamic chamber technique was used to measure ground layer CO_2 fluxes, ecosystem photosynthesis (GEP), total ecosystem respiration (ER) and net ecosystem exchange (NEE) every second week from each collar in 2016 (May to September) and 2017 (May to August). A transparent plastic closed chamber was used to measure CO_2 concentration, temperature, humidity and PAR at the interval of 15 sec for 2 min by using an infrared gas analyzer system (EGM-4, PP$_{Systems}$).

Annual carbon fluxes were estimated by following Bravo et al. (2018), Günther et al. (2015) and Strack et al. (2018) as follows:

$$NECB \ (g \ C \ m^{-2} \ yr^{-1}) = NEE + NPP + LITTER + CH_4 - R_{tree}$$

Where, NECB is net ecosystem carbon balance, NEE stands for the net ecosystem exchange of carbon from understory vegetation, NPP is net primary production of trees/shrubs including both aboveground and belowground carbon, CH_4 is annual methane flux, and R_{tree} stands for the tree root respiration. Here we include litter with NPP when reporting results as we calculated fen overstory NPP including leaf (litter) biomass.

Results and discussion
In 2016, the ground layer of the bog was a source (1.66 g CO_2 m^{-2} d^{-1}) and fen was a sink (-19.06 g CO_2 m^{-2} d^{-1}) of CO_2. However, in 2017, both bog and fen were a sink of CO_2 (-1.35 g CO_2 m^{-2} d^{-1} and -19.06 g CO_2 m^{-2} d^{-1} respectively). The CH_4 flux from the bog in 2017 (171.67 mg CH_4 m^{-2} d^{-1}) was significantly higher than in 2016 (56.43 mg CH_4 m^{-2} d^{-1}, $p < 0.005$). However, in the fen, no significant CH_4 differences were observed in both 2016 and 2017.

Overall, in both 2016 and 2017, the bog upstream was greater source of CH_4 compared to the downstream, in HI areas. However, in LI areas, the downstream was greater source of CH_4 than the upstream. This could be due to the observed shallower water table on the downstream areas of the bog (Table 13). Also, in the bog, significantly more CH_4 was emitted by areas closer to the road (Table 13), where the water table was shallower, but no significant variation was observed at the fen by the road distance factor (Table 14). In both bog and fen, a significant positive correlation was observed between CH_4 flux and water table position, and CH_4 flux and peat temperature. Also, the N_2O emissions from bog and fen were negligible in 2016 and 2017. Fluxes of CH_4 were fairly high in the non-growing season, but were measured in an abnormally warm period in winter 2015 (Table 15).

Table 13: CO_2 and CH_4 fluxes from a bog in Carmon Creek, Peace River, Alberta, 2016 and 2017[a].

Culvert distance	Side of the road	Distance from road (m)	CO_2 flux $g\ CO_2\ m^{-2}\ d^{-1}$			CH_4 flux $mg\ CH_4\ m^{-2}\ d^{-1}$
			2016			
			NEE	**GEP**	**ER**	**CH₄**
50 m			-1.10 ± 1.28	-12.93 ± 1.88	11.83 ± 1.74	4.05 ± 1.63
> 20 m	**Upstream**	2	3.66 ± 1.43	-3.35 ± 0.72	7.01 ± 1.55	305.61 ± 97.48
		6	1.95 ± 1.22	-4.08 ± 0.50	6.03 ± 1.16	52.45 ± 15.36
		20	-2.85 ± 1.70	-12.27 ± 1.61	9.42 ± 0.90	15.85 ± 2.99
	Downstream	2	1.34 ± 1.94	-14.56 ± 2.07	15.90 ± 2.52	17.85 ± 8.68
		6	-5.5 ± 1.51	-17.40 ± 1.94	12.05 ± 1.52	2.54 ± 0.83
		20	-3.90 ± 2.32	-19.94 ± 2.47	16.03 ± 1.63	4.63 ± 1.59
< 2 m	**Upstream**	2	-1.23 ± 1.28	-10.61 ± 1.89	9.38 ± 1.64	77.41 ± 20.47
		6	-0.16 ± 0.72	-5.43 ± 0.97	5.27 ± 0.7	75.85 ± 22.76
		20	-1.0 ± 1.70	-10.35 ± 1.32	9.34 ± 1.27	18.31 ± 9.98
	Downstream	2	11.80 ± 2.02	-17.12 ± 1.98	28.93 ± 2.73	31.44 ± 12.08
		6	6.64 ± 2.96	-22.72 ± 2.56	29.35 ± 2.57	22.06 ± 10.04
		20	8.18 ± 2.70	-19.23 ± 2.0	27.41 ± 3.44	23.35 ± 11.04
			2017			
50 m			-1.11 ± 1.63	-17.64 ± 1.23	16.53 ± 1.48	9.62 ± 3.37
> 20 m	**Upstream**	2	4.37 ± 2.77	-8.47 ± 1.80	12.84 ± 3.20	890.89 ± 287.70
		6	-4.96 ± 2.64	-15.33 ± 3.00	10.37 ± 0.92	160.56 ± 22.24
		20	0.05 ± 1.65	-6.70 ± 1.70	6.75 ± 0.51	68.69 ± 46.51
	Downstream	2	-0.40 ± 1.92	-17.38 ± 2.0	16.99 ± 1.82	10.13 ± 2.26
		6	-3.01 ± 1.64	-17.82 ± 1.90	14.82 ± 1.50	7.50 ± 1.69
		20	-8.33 ± 2.29	-24.51 ± 2.38	16.18 ± 1.35	7.77 ± 2.37
< 2 m	**Upstream**	2	-6.14 ± 1.61	-23.99 ± 2.85	17.84 ± 2.33	173.75 ± 69.04
		6	-6.47 ± 2.34	-18.40 ± 3.38	11.93 ± 1.74	176.52 ± 40.82
		20	-0.60 ± 1.29	-8.28 ± 1.99	7.68 ± 1.40	17.50 ± 4.59
	Downstream	2	9.54 ± 2.49	-20.19 ± 1.92	29.73 ± 2.78	68.56 ± 18.42
		6	2.59 ± 3.84	-27.39 ± 3.19	29.99 ± 3.07	310.29 ± 242.84
		20	-1.27 ± 2.86	-22.86 ± 2.46	21.58 ± 2.14	31.03 ± 10.65

a. All values are given as mean of three plots $\pm$ standard error and represent only the understory fluxes

Table 14: CO_2 and CH_4 fluxes from a fen in Carmon Creek, Peace River, Alberta, 2016 and 2017[a].

Culvert distance	Side of the road	Distance from road (m)	CO₂ flux g CO₂ m⁻² d⁻¹			CH₄ flux mg CH₄ m⁻² d⁻¹
2016						
			NEE	GEP	ER	CH₄
50 m			-19.82 ± 2.68	-39.95 ± 3.86	20.13 ± 2.23	5.11 ± 1.28
> 20 m	**Upstream**	2	-13.31 ± 3.55	-31.51 ± 3.98	18.20 ± 1.87	7.96 ± 1.85
		6	-15.58 ± 3.96	-31.47 ± 4.63	15.89 ± 3.09	6.37 ± 1.66
		20	-18.89 ± 3.78	-43.73 ± 4.06	24.84 ± 2.38	6.20 ± 1.89
	Downstream	2	-21.44 ± 3.66	-52.0 ± 3.89	30.56 ± 3.09	5.91 ± 1.61
		6	-20.59 ± 3.11	-48.45 ± 3.60	27.87 ± 2.87	12.95 ± 4.42
		20	-15.90 ± 2.36	-45.38 ± 4.00	29.48 ± 2.59	10.13 ± 3.57
< 2 m	**Upstream**	2	-27.55 ± 3.31	-49.82 ± 4.07	22.27 ± 3.37	9.15 ± 3.61
		6	-10.87 ± 3.80	-27.66 ± 3.36	16.79 ± 3.26	6.14 ± 1.88
		20	-18.10 ± 3.25	-35.63 ± 4.19	16.64 ± 1.96	4.39 ± 1.18
	Downstream	2	-25.27 ± 3.54	-49.70 ± 4.84	24.43 ± 2.45	4.67 ± 1.63
		6	-16.26 ± 3.34	-52.29 ± 4.75	28.55 ± 3.30	9.08 ± 2.37
		20	-23.74 ± 4.49	-38.85 ± 4.19	22.58 ± 2.63	4.98 ± 1.71
2017						
50 m			-7.89 ± 3.67	-35.04 ± 4.64	27.15 ± 3.50	34.04 ± 23.58
> 20 m	**Upstream**	2	-14.30 ± 2.42	-42.17 ± 4.16	27.87 ± 3.10	5.44 ± 0.97
		6	-6.58 ± 2.57	-30.11 ± 4.35	23.52 ± 2.91	8.56 ± 3.86
		20	-13.97 ± 3.06	-49.08 ± 3.63	35.11 ± 3.04	12.34 ± 3.11
	Downstream	2	-12.02 ± 4.42	-40.15 ± 5.27	28.13 ± 3.87	49.55 ± 37.92
		6	-6.67 ± 3.85	-39.32 ± 4.62	32.65 ± 3.20	11.07 ± 4.59
		20	-4.69 ± 2.56	-39.74 ± 4.89	35.07 ± 3.45	13.56 ± 4.76
< 2 m	**Upstream**	2	-12.31 ± 4.01	-47.10 ± 4.96	34.79 ± 4.93	19.14 ± 5.79
		6	-31.71 ± 21.14	-127.08 ± 84.96	95.37 ± 64.04	7.73 ± 2.58
		20	-10.39 ± 3.03	-33.13 ± 4.40	22.74 ± 3.42	10.31 ± 4.07
	Downstream	2	-20.71 ± 3.31	-55.44 ± 6.00	34.73 ± 3.97	12.69 ± 1.98
		6	-3.63 ± 5.31	-37.67 ± 4.90	34.03 ± 4.18	16.75 ± 6.40
		20	-12.47 ± 5.20	-39.32 ± 5.56	26.86 ± 2.82	7.77 ± 3.45

a.   All values are given as mean of three plots ± standard error and represent only the understory fluxes.

We determined NECB by combining ground layer fluxes with overstory NPP (Tables 16 and 17). Both the bog and fen were sinks of carbon in areas greater than 50 m from the road, with a greater sink at the fen. Close to the road, carbon sink strength was reduced at both sites. At the bog, many areas close to the road were converted to net sources of carbon.

Lessons learned

Road crossings in peatland can alter GHG and C exchange. Areas with greater hydrologic impact are likely to have the greatest alteration to GHG emissions. Culverts reduce the impact of flooding in upgradient areas on tree productivity and CH_4 emissions, but can result in localized flooding on the downgradient side if they are spaced a great distance apart. This can result in reduced tree productivity and enhanced CH_4 emissions near culverts on the downgradient side of the road.

Table 15: Non-growing season CH_4 fluxes from a fen and a bog in Carmon Creek, Peace River, Alberta, 2015.

Disturbed/ Reference areas	Factors			Mean CH_4 flux mg CH_4 m^{-2} day^{-1} ± SE	
	Culvert position	Side of the road	Distance from the road (m)	Bog	Fen
≤ 20 m				5.8 ± 2.04	4.05 ± 0.27
50 m				16.03 ± 1.34	2.50 ± 0.39
≤ 20 m		Upstream		4.41 ± 1.75	5.98 ± 0.21
		Downstream		7.19 ± 2.18	2.12 ± 0.33
	> 20 m			5.22 ± 1.88	3.96 ± 0.31
	< 2 m			6.38 ± 2.19	4.13 ± 0.22
			2	6.19 ± 2.00	5.40 ± 0.28
			6	5.78 ± 2.30	4.22 ± 0.58
			20	5.44 ± 1.80	2.52 ± 0.54

Table 16: Net ecosystem carbon balance (NECB) at the bog site

Culvert distance	Side of road	Distance from road	CO$_2$ flux	CH$_4$ flux	NECB
2016			g C m^{-2} yr^{-1}		
	50 m (control)		-314.7 ± 76.6	0.8 ± 0.1	-313.9 ± 76.5
>20 m	Upstream	2	198.7 ± 47.3	48.3 ± 21.7	247.0 ± 35.5
		6	6.2 ± 221.9	6.2 ± 2.6	12.3 ± 222.9
		20	-57.2 ± 106.0	2.1 ± 0.5	-55.1 ± 106.4
	Downstream	2	-8.9 ± 198.8	0.9 ± 0.4	-8.0 ± 198.4
		6	-264.4 ± 103.3	0.4 ± 0.3	-264.0 ± 103.1
		20	-256.6 ± 98.5	0.4 ± 0.3	-256.2 ± 98.8
< 2 m	Upstream	2	-101.1 ± 190.3	7.8 ± 2.5	-93.2 ± 187.8
		6	130.3 ± 254.9	8.2 ± 1.2	138.5 ± 254.1
		20	-13.6 ± 89.3	2.0 ± 1.1	-11.6 ± 89.6
	Downstream	2	317.2 ± 142.6	3.6 ± 1.6	320.8 ± 144.0
		6	250.2 ± 240.0	3.8 ± 2.2	254.0 ± 242.2
		20	24.2 ± 309.3	1.8 ± 1.1	25.9 ± 309.8
2017					
	50 m (control)		-201.3 ± 60.8	0.9 ± 0.2	-200.4 ± 60.9
>20 m	Upstream	2	99.3 ± 123.6	116.9 ± 113.2	216.2 ± 210.9
		6	57.0 ± 225.6	22.8 ± 11.3	79.8 ± 225.9
		20	-168.2 ± 89.8	3.9 ± 1.3	-164.3 ± 90.9
	Downstream	2	-218.5 ± 191.3	0.6 ± 0.2	-217.9 ± 191.5
		6	-161.5 ± 174.8	0.8 ± 0.2	-160.8 ± 174.7
		20	-400.2 ± 38.7	1.4 ± 0.5	-398.9 ± 38.3
< 2 m	Upstream	2	-133.2 ± 178.6	35.8 ± 18.8	-97.4 ± 176.9
		6	-80.3 ± 384.1	22.6 ± 7.9	-57.8 ± 378.3
		20	-210.6 ± 204.1	2.9 ± 1.8	-207.6 ± 202.4
	Downstream	2	13.8 ± 308.4	10.9 ± 4.8	24.6 ± 304.8
		6	23.1 ± 291.4	9.6 ± 4.2	32.7 ± 295.5
		20	-158.2 ± 275.7	6.0 ± 2.3	-152.2 ± 274.6

Table 17: Net ecosystem carbon balance (NECB) at the fen site

Culvert distance	Side of road	Distance from road	CO$_2$ flux	CH$_4$ flux	NECB
2016			g C m^{-2} yr^{-1}		
	50 m (control)		-900.2 ±102.8	0.6 ± 0.6	-899.6 ± 102.7
>20 m	Upstream	2	-1814.8 ± 1108.9	0.8 ± 0.3	-1814.0 ± 1109.1
		6	-744.0 ± 184.3	1.6 ± 0.3	-742.4 ± 184.4
		20	-805.3 ± 155.0	1.4 ± 0.7	-803.9 ± 155.5
	Downstream	2	-1248.6 ± 223.7	0.8 ± 0.2	-1247.6 ± 223.6
		6	-849.5 ± 143.3	1.0 ± 0.2	-848.7 ± 143.5
		20	-527.3 ± 114.8	0.8 ± 0.3	-526.6 ± 115.0
< 2 m	Upstream	2	-695.4 ± 322.2	0.9 ± 0.2	-694.4 ± 322.4
		6	-901.5 ± 339.9	1.0 ± 0.2	-900.5 ± 339.7
		20	-805.1 ± 259.2	0.9 ± 0.4	-804.2 ± 259.4
	Downstream	2	-599.8 ± 284.2	1.3 ± 0.5	-598.4 ± 284.7
		6	-1005.4 ± 103.3	0.7 ± 0.3	-1004.8 ± 103.4
		20	-735.5 ± 59.8	0.7 ± 0.4	-734.8 ± 59.4
2017					
	50 m (control)		-729.8 ± 112.2	3.0 ± 1.3	-726.8 ± 112.5
>20 m	Upstream	2	-336.9 ± 115.2	4.3 ± 3.2	-335.8 ± 115.1
		6	-324.9 ± 130.2	1.6 ± 0.7	-323.3 ± 129.6
		20	-601.3 ± 82.2	2.0 ± 0.3	-599.3 ± 82.0
	Downstream	2	-177.7 ± 248.5	1.8 ± 0.9	-176.0 ± 249.2
		6	-57.8 ± 429.1	1.7 ± 0.4	-55.4 ± 429.1
		20	-76.0 ± 125.4	2.4 ± 0.4	-74.7 ± 125.4
< 2 m	Upstream	2	-341.4 ± 119.3	0.9 ± 0.3	-340.5 ± 119.0
		6	-607.4 ± 130.5	3.4 ± 2.7	-604.0 ± 130.7
		20	-332.4 ± 165.3	0.8 ± 0.4	-331.6 ± 165.0
	Downstream	2	-492.9 ± 248.6	2.3 ± 0.8	-490.6 ± 249.1
		6	-340.8 ± 221.5	1.3 ± 0.6	-339.5 ± 221.6
		20	-451.0 ± 30.7	1.6 ± 0.6	-449.4 ± 30.2

3. Greenhouse Gas and Non-GHG impacts

This study is the first to quantify the effect of permanent linear disturbances (PLD), in this case access roads, on peatland GHG exchange. We observed that the effect of road crossings in peatlands is site specific, depending on the direction of the road crossing relative to the topography in the peatland, and not necessarily the peatland type. When the road crosses perpendicular to the slope, hydrological effects, and from that induced GHG emissions, are greater. The hydrological and land-cover changes induced by the road crossing alter both CO_2 and CH_4 fluxes from the peatland in areas within 20-40 m from the road with a decline in CO_2 uptake and increase in CH_4 flux. A reduction in CO_2 uptake occurs close to the road, regardless of hydrological impact, due to removal and thinning of overstory vegetation during road construction and use. Culverts can

mitigate some of the hydrologic impact, but at our site, the culverts would need to be spaced closer than 20 m to be most effective. We have observed that when culverts are isolated, their impact may be to enhance GHG emissions by increasing CH_4 emissions on the downgradient side of the road. Because water flow becomes concentrated through the culverts water table rises on both up- and downgradient sides of the road.

Table 18: Calculated GHG impact of road crossings at study peatlands

Site	0 – 40 m from road[a]			Control (> 50 m from road)			Road effect[c]
	CO_2 flux (g C m^{-2} yr^{-1})	CH_4 flux (g C m^{-2} yr^{-1})	GWP[c] (g CO$_2$-e m^{-2} yr^{-1})	CO_2 flux (g C m^{-2} yr^{-1})	CH_4 flux (g C m^{-2} yr^{-1})	GWP (g CO$_2$-e m^{-2} yr^{-1})	
Fen Culvert <2 m	-600[b] (-890 to -360)	1.2 (0.4 to 2.3)	-2160 (-3240 to -1280)	-630 (-1010 to -410)	1.4 (0.3 to 2.4)	-2270 (-3670 to -1450)	180 (-240 to 650)
Fen culvert >20 m	-520 (-190 to -810)	1.5 (0.9 to 2.3)	-1840 (-2920 to -650)				330 (-210 to 1060)
Bog culvert <2 m	-70 (-330 to 170)	6.5 (2.7 to 8.4)	-10 (-670 to 730)	-260 (-1020 to -100)	0.8 (0.3 to 1.1)	-910 (-3740 to -330)	900 (30 to 1850)
Bog culvert >20 m	-160 (-270 to -10)	7.0 (1.8 to 25)	-310 (-920 to 190)				600 (-210 to 1280)

a. Calculations are based on measurements at 2, 6, and 20 m from the road on both up and downgradient sides, applied to the area from 0 to 40 m.
b. High levels of variation are due to large spatial variability in fluxes (i.e., between microforms) that were specifically targeted in sampling design to ensure that mean represented average shift in overall site conditions.
c. Road effect is expressed in global warming potential (GWP) where positive values indicate that the road has reduced peatlands' greenhouse gas sink and/or increased release.

We calculated the potential impact of our study sections of roads on GHG emissions within 40 m of the road on both sides of the road using data from both study years (values presented in section 2.10). We calculated a weighted average GHG emission with values measured at 2 m were applied, on the appropriate side of the road, to an area 0-4 m from the road, values measured at 6 m, from an area 4-14 m from the road, and values measured at 20 m, from 14-40 m. This average GHG flux was compared to average flux measured in the control areas (more than 50 m from the road) and the difference given as the road impact. We express the GHG impact as a global warming potential (GWP) in g CO_2 equivalents (CO$_2$-e) where each gram of CH_4 is assigned a GWP of 28 times CO_2 (Myhre et al., 2013). We observed that at the fen, where hydrological impacts were minimal, the site remained on average a GHG sink (Table 18) although this was reduced both close to and far from culverts. The reduction in GHG sink was largely due to a reduction in CO_2 uptake that appears linked to vegetation disturbance close to the road (Figure 14). At the bog, the road impacted area also remained a GHG sink, but this sink was reduced by both reduced CO_2 uptake and increased CH_4 emissions. The latter was driven by hydrological impacts, and the increase in CH_4 flux was actually greater at areas with culverts due to increased inundation downgradient of the road where culverts discharged water (Figure 14). Therefore, we found no mitigating effect of the culverts on the GHG impact of the road. While this study demonstrates the potential GHG

impact of peatland road crossings, many more sites are needed before results can be generalized to all cases.

Although culverts did not mitigate GHG emissions in this specific case, it is likely that at an appropriate density, culvert could mitigation emissions. However, installation of culverts requires additional machine time during road construction that will induce GHG emissions. Discussions with the industry partner indicate that culvert installation involves additional machine time to install the culvert (deeper excavation below the culvert and compaction of clay), as well as truck time to transport the clay placed beneath the culvert and the culvert itself. Altogether, they estimate ~ 8 hours additional machine time per culvert. We divided this evenly between truck time (4 hours) and excavator time (4 hours). Using average hourly fuel use of vehicles in quarry operations (Klanfar et al., 2016) and emission factors for diesel fuel used in Canada's national inventory report (ECCC, 2018), we estimate total GHG emissions for installation of one culvert at 548 kg CO_2-e of which CH_4 accounts for <0.1% of the total.

The goal of this study was not to construct many new roads to systematically reduce peatland GHG emissions. However, the results from this study can be used to better quantify the GHG impact of current peatland PLD crossings and ensure more effective culvert placement in future. Our findings clearly indicate that mitigating GHG impacts of roads requires a reduction in vegetation disturbance near the road during road construction and effective mitigation of hydrologic impacts. The latter requires distributed hydrologic connection across the disturbance, particularly when the road crosses perpendicular to the peatland slope. The lessons learned here should also encourage industry to test innovative road construction strategies and monitor their effectiveness in reducing vegetation and hydrologic impacts. In support of this effort, this project has also developed a suite of remote sensing tools applicable to mapping conditions in peatlands. We have demonstrated the ability of UAV photogrammetry to measure peatland microtopography and water table position, even in treed peatlands, and to estimate shrub biomass. This paves the way for the use of geospatial methods in peatland disturbance monitoring and GHG estimation.
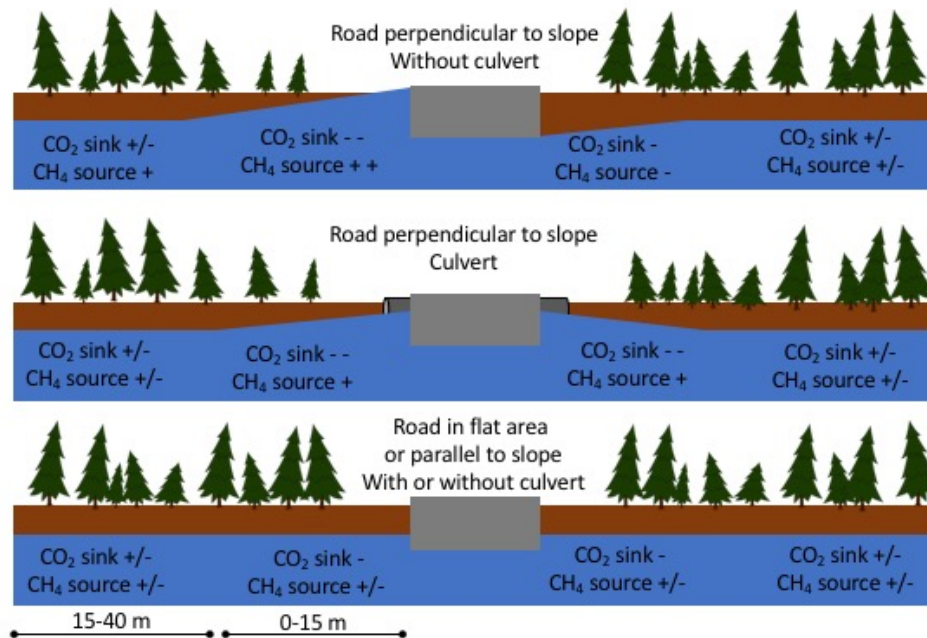
Figure 14: Summary of road crossing impacts on peatland GHG fluxes as observed in the present study. Signs beside flux indicate direction and relative magnitude of change: +/- indicates little to no change in direction or magnitude, + indicates small increase, - indicates small decrease, ++ indicates large increase, -- indicates large decrease.

Furthermore, while conducting this study we were able to begin to estimate the potential impact of seismic lines on peatland GHG exchange, identifying a potentially important additional land-use GHG emission, beginning the steps needed to develop methods to estimate the GHG impact of this disturbance that could be applied to provincial or national scale reporting and identify important knowledge gaps on the impacts of disturbance to wetland GHG exchange.

Finally, through this project we have trained one research associate, one PhD student, two MSc students and seven undergraduate students with technical skills related to peatland GHG exchange, hydrology, vegetation survey, topographic surveys, UAV operation and image interpretation, field safety, scientific communication and stakeholder engagement. While some are still completing their studies, several of these trainees have moved on to positions supporting academic research on resource management and environmental consulting.

4. Overall Conclusions

Road crossings in peatlands reduce the GHG sink of these ecosystems due to vegetation disturbance adjacent to the road and hydrologic impacts when the road crosses perpendicular to the slope of the land. Widely spaced culverts were ineffective at mitigating GHG impacts and appear to result in greater GHG sink reductions. This results from concentration of water flow that increases CH_4 emissions on both sides of the road crossing. Future research should focus on road construction techniques that create distributed hydrologic connection; this may be achievable by closely spaced culverts, but also likely requires new techniques such as permeable fills or subsurface drains. We have developed a suite of geospatial tools that will be useful to monitor the

success of future road constructions projects in mitigating vegetation and hydrological disturbances, and hence GHG impacts, in peatlands.

5. Scientific Achievements

In all publications below, trainees from the project are underlined.

5.1. Student theses

Fanson, J. 2017. An examination of plant biomass and the effects of road construction on forested bog. B.Sc. research project, University of Calgary, Calgary, AB

Lovitt, J. 2017. Quantifying the impact of seismic lines on methane release in a treed bog ecosystem using unmanned aerial vehicles (UAVs). MSc Thesis, University of Calgary, Calgary, AB.

He, A. 2019. Mapping shrub biomass in a boreal continental fen. MSc Thesis, University of Calgary, Calgary, AB.

Wrubleski, M. 2017. Do roads built through northern peatland impact dissolved organic carbon cycling? B.Sc. honours thesis. University of Calgary, Calgary, AB.

5.2. Presentations

Fanson, J., Saraswati, S., Strack, M. 2017. The effects of road construction on plant biomass in a forested bog. NAIT 7th Annual Seminar: Linear Disturbance Impacts on Boreal Wetland Ecosystems - November 16.

He, A., McDermid, G., Rahman, M.M. 2018. Mapping aboveground biomass using unmanned aerial vehicles in a boreal continental peatland. ESA Annual Meeting – August 5-10, 2018, New Orleans, Louisiana, USA.

He, A., Rahman, M.M., McDermid, G. 2017. The application of Unmanned Aerial Vehicle (UAVs) with estimating aboveground biomass in Alberta's peatlands. NAIT 7th Annual Seminar: Linear Disturbance Impacts on Boreal Wetland Ecosystems - November 16, 2017.

Lovitt, J., Rahman, M.M., McDermid, G. 2017. Mapping the microtopography of a complex forested bog in Alberta using Unmanned Aerial Vehicles (UAVs). NAIT 7th Annual Seminar: Linear Disturbance Impacts on Boreal Wetland Ecosystems - November 16, 2017.

Lovitt, J., Rahman, M.M., McDermid, G. 2017. Mapping Micro-Topography of Peatlands within Alberta: Applications for Unmanned Aerial Vehicle (UAV) Technology. Earth Observation Summit 2017. 20-22 June, Montreal, QC Canada.

McDermid, G., Lovitt, J., Rahman, M.M., Strack, M., Xu, B. 2018. UAVs Reveal the Effects of Seismic Lines on Surface Morphology, Water Table Position, and Methane Emissions in Boreal Peatlands. Canadian Symposium on Remote Sensing – June 18-21, 2018, Saskatoon, SK, Canada.

Rahman, M.M., McDermid, G., Strack, M. 2018. A new workflow to remove shadow from UAV imagery with a view to improve vegetation structure delineation in a classical bog. ESA Annual Meeting – August 5-10, 2018, New Orleans, Louisiana, USA

Rahman, M.M., McDermid, G., 2018. UAV data processing – a strategy to improve point cloud and orthomosaic by removing shadow. Canadian Symposium on Remote Sensing – June 18-21, 2018, Saskatoon, SK, Canada.

Rahman, M.M., McDermid, G., Lovitt, J., Strack, M. Xu, B. 2017. Estimating depth to groundwater table in a disturbed peatland in Alberta using photogrammetric point clouds. NAIT 7th Annual Seminar: Linear Disturbance Impacts on Boreal Wetland Ecosystems - November 16, 2017.

Rahman, M.M., McDermid, G., Lovitt, J., Strack, M. Xu, B. 2017. Mapping Peat Groundwater Table Dynamics using Unmanned Aerial Vehicle and Photogrammetric Techniques. Earth Observation Summit 2017. 20-22 June, Montreal, QC Canada

Rahman MM, McDermid G, Lovitt J. 2017. Estimating depth to groundwater table in a disturbed peatland in Alberta using photogrammetric point clouds. COSIA Innovation Summit, Calgary, AB, March 21.

Saraswati, S., Strack. M., Petrone, R., Rahman, M.M., McDermid, G., Xu, B.. 2018. Impacts of a road on a hydrological connection of forested boreal peatlands, American Geophysical Union, Washington, DC, USA, December 10.

Saraswati, S., Strack, M., Parsons, C.. 2018. Impacts of access roads on enzyme activities of boreal forested peatlands, Canadian Geophysical Union Joint meeting, Niagara Fall, Ontario, Canada, June 11.

Saraswati, S., Strack, M. 2018. How do access roads impact hydrology, enzyme activities and GHG emissions from boreal peatlands? Canadian Geophysical Union Annual Student Meeting 2018, Western University, London, Canada, March 17.

Saraswati, S., Strack, M. 2018. Impact of access roads on GHGs emission from boreal peatlands, World Wetlands Day 2018, The University of Waterloo, Ontario, Canada, February 2.

Saraswati, S., Strack, M., Petrone, R., Rahman, M.M., McDermid, G., Xu, B. 2018. Comparing access road impacts on boreal peatlands' hydrological connections between wet and dry years, Canadian Geophysical Union Joint meeting, Niagara Falls, ON, June 11.

Saraswati, S., Strack, M., Petrone, R., Rahman, M.M., McDermid, G., Xu, B. 2018. Mitigating hydrological impacts on GHG emission induced by resource access roads crossing forested boreal peatlands, COSIA Innovation Summit, Calgary, Canada, June 8.

Saraswati, S., Strack, M. 2017. Can access roads impact carbon dynamics of boreal forested peatlands by altering enzyme activities, 11th The North American Forest Ecology Workshop, The University of Albert, Edmonton, Alberta, Canada, June 19.

Saraswati, S., Strack, M.. 2016. Road induced Greenhouse gas emissions from boreal peatlands and potential for mitigation, Worlds Wetland Day, Waterloo University, Canada, February 2.

Saraswati, S., Strack, M. 2016. Road induced Greenhouse gas emissions from boreal peatlands and potential for mitigation, Alberta Soil Science Workshop, Canada, February 16.

Strack, M. 2018. Cutting across the boreal: linear disturbance impact on peatland carbon exchange. Geography Speaker Series, Western University, London, ON. September 28.

Strack, M. 2018. A line in the peat: The impact of linear disturbances on boreal peatland ecosystems. Biology Seminar, Laurentian University, Sudbury, ON, March 23.

Strack, M., Kostic, A, McDermid, G., Rahman, M., Saraswati, S., Xu, B. 2018. The impact of seismic lines on boreal peatland methane emissions. Canadian Geophysical Union Joint meeting, Niagara Falls, ON. June 11.

Strack, M. 2016. Oil exploration and extraction in Canada's boreal region: Impacts and restoration on peatland ecosystems. Swedish Agricultural University (SLU), Uppsala, Sweden, October 26.

Strack M, Saraswati S, Xu B, Rahman MM, Lovitt J, McDermid G. 2017. Mitigating greenhouse gas emissions induced by road crossings in boreal peatlands, COSIA Innovation Summit, Calgary, AB, March 21.

Wrubleski, M., Saraswati, S., Strack, M. 2017. How roads impact dissolved organic carbon concentrations. NAIT 7th Annual Seminar: Linear Disturbance Impacts on Boreal Wetland Ecosystems - November 16.

5.3. Journal publications

He, A., McDermid, G.J., Rahman, M.M., Strack, M., Saraswati, S., Xu, B. 2018. Developing allometric equations for estimating shrub biomass in a boreal fen. *Forests*, 9: 569, doi: 10.3390/f9090569.

He, A., McDermid, G., Rahman, M., Strack, M., Saraswati, S., & Xu, B. 2019. UAV and photogrammetric techniques for estimating shrub biomass in a boreal fen (in preparation).

Lovitt J, Rahman MM, McDermid G. 2017. Assessing the value of UAV photogrammetry for characterizing terrain in complex peatlands. Remote Sensing, 9, 715, doi: 10.3390/rs9070715

Lovitt, J., Rahman, M., Saraswati, S., McDermid, G.J., Strack, M**.,** Xu, B. 2018. UAV remote sensing can reveal the effects of low impact seismic lines on methane (CH_4) release in a forested boreal bog. *Journal of Geophysical Research*, 123, doi: 10.1002/2017JG004232.

Rahman, M.M., McDermid, G., Mckeeman, T., Lovitt, J. 2019. A workflow to minimize shadow in UAV-based orthomosaics. Journal of Unmanned Vehicle Systems, doi: 10.1139/juvs-2018-0012

Rahman, M.M., McDermid, G. Strack, M., Lovitt, J. 2017. A new method to map groundwater table in peatlands using unmanned aerial vehicles, *Remote Sensing*, 9, 1057, doi: 10.3390/rs9101057.

Rahman, M.M., Strack, M., McDermid, G.J. in preparation. Introducing mineral road in a peatland alters land cover.

Saraswati, S., Parsons, C.T., Strack, M. 2019. Access roads impact enzyme activities in boreal forests peatlands. *Science of the Total Environment*, 651: 1405-1415.

Strack, M., Hayne, S., Lovitt, J., McDermid, G.J., Rahman, M.M., Saraswati, S., Xu, B. revision submitted. Petroleum exploration increases methane emissions in northern peatlands. *Nature Communications*.

6. Next Steps

The present study determined the effect of peatland road crossings on local GHG emissions at two peatlands and the potential of culverts to mitigate this effect. At both study sites the roads were <5 years old at the end of the study and more research is needed to determine the longer term effects of roads on peatland carbon and GHG exchange. Moreover, results from this study suggest that widely spaced culverts are not effective at mitigating road induced GHG emissions, indicating that studies on other construction practices are required. We have determined the importance of hydrological conditions and overstory productivity for driving resultant GHG emissions and developed geospatial tools to measure and map these factors spatially. This opens the door for future studies across many more sites where GHG emissions can be inferred from changes in ecohydrological conditions.

The research team will continue to disseminate research results from the project in scientific literature, conference presentations and stakeholder engagement. We plan for several more peer-reviewed publications based on the results of the project including: 1) land cover change in peatlands affected by roads, 2) hydrological impacts of peatland road crossings, 3) effect of peatland roads on tree productivity, 4) UAV photogrammetry for shrub biomass estimation, 5) effect of peatland road crossings on carbon and greenhouse gas exchange. We will also continue to share results from the project at scientific meetings (e.g., Canadian Geophysical Union, European Geophysical Union) and workshops.

The research team plans to continue investigating disturbance impacts to peatland GHG exchange through several ongoing and proposed projects. The team has started pilot projects to measure GHG exchange directly on peatland seismic lines and test WT mapping techniques developed in this project at other study sites. Building on this work, the research team is developing a research proposal, with government scientists at Canadian Forest Service and Environment and Climate Change Canada that will extend the work in the present study and aims to improve estimates of anthropogenic disturbance impacts (including roads and seismic lines) on peatland GHG emissions at regional and national scales.

7. Communication Plan

A major objective of the project was communication of results to stakeholders in order to improve future road construction. This has been completed partially through presentation of results at a range of venues reaching academic, industry, government and non-governmental organizations (e.g., scientific conference, industry workshops such as COSIA Innovation Summit, training seminars).

In addition, in collaboration with Ducks Unlimited Canada and Alberta Biodiversity Monitoring Institute, we organized a workshop entitled "Linear Disturbance Impacts to Boreal Wetland Ecosystems". This workshop was hosted at NAIT's Edmonton campus on November 16, 2017. The workshop included presentations by our project leads (Strack, McDermid, Xu) focused on three themes: 1) mapping linear disturbances, 2) impacts of linear disturbances on wetland function, and 3) restoration of wetland linear disturbances. Each presentation was followed by a series of "lightning" presentations by relevant speakers, followed by poster sessions where more in depth discussions took place. The afternoon session was organized as a break-out session in which participants discussed research gaps and opportunities related to each of the workshop themes. Approximately 60 participants took part representing universities, provincial and federal government departments, forestry and oil industries, NGOs and environmental consulting firms. In addition to disseminating project results to relevant stakeholder at the workshop, all presentations have been published on the NAIT Boreal Research Institute website (http://www.nait.ca/103609.htm) creating a resource available to those unable to attend.

Results have also been communicated in peer-reviewed literature (see Scientific Achievements) and we have generally made these results available in open access journals. In cases where the journal article is not open access, post-prints will be placed in the University of Waterloo's open access repository UWSpace (https://uwspace.uwaterloo.ca) according to journal embargo regulations. We plan to continue disseminating results not yet published according to these guidelines as the manuscripts are finalized.

Moving forward, the project team maintains strong collaborative relationships with government departments, industry and NGOs and will continue to share knowledge and data developed through the research program to better quantify disturbance effects to peatland GHGs and implement practices to mitigate these impacts. For example, in November 2018, Xu and Strack participated in a workshop at Canadian Forest Service to develop disturbance matrices related to modeling disturbance impacts on peatland carbon and GHG exchange for use in national managed forest GHG quantification.

8. References

Abdalla, M., Hastings, A., Truu, J., Espenberg, M., Mander, Ü., & Smith, P. (2016). Emissions of methane from northern peatlands: a review of management impacts and implications for future management options. *Ecology and evolution*, *6*(19), 7080-7102.

Alberta Biodiversity Monitoring Institute (AMBI). *Enhanced Linear Features in the Oil Sands Region 2014* (Alberta Biodiversity Monitoring Institute, Edmonton, AB, Canada, 2017).

Alberta Environment and Parks. *Alberta Merged Wetland Inventory:* https://geodiscover.alberta.ca/geoportal/catalog/search/resource/details.page?uuid=%7BA73F5A E1-4677-4731-B3F6-700743A96C97%7D (accessed September 29, 2017)

Badiou, P., Page B (2014) Wetland Road Crossing Hydrological Monitoring Design and Data Summary. Ducks Unlimited Canada, Final Report Prepared for Conservation and Community Grants Program.

Box, J. D. (1983). Investigation of the Folin-Ciocalteau phenol reagent for the determination of polyphenolic substances in natural waters. *Water research*, *17*(5), 511-525.

Cresto-Aleina, F., Runkle, B. R. K., Kleinen, T., Kutzbach, L., Schneider, J., & Brovkin, V. (2015). Modeling micro-topographic controls on boreal peatland hydrology and methane fluxes. *Biogeosciences*, *12*, 5689-5704.

Dabros, A., Pyper, M., & Castilla, G. (2018). Seismic lines in the boreal and arctic ecosystems of North America: environmental impacts, challenges, and opportunities. *Environmental Reviews*, *26*(2), 214-229.

Dunn, C., Jones, T. G., Girard, A., & Freeman, C. (2014). Methodologies for extracellular enzyme assays from wetland soils. *Wetlands*, *34*(1), 9-17.

ECCC (2018). National Inventory Report 1990 – 2016: Greenhouse gas sources and sinks in Canada. Environment and Climate Change Canada, Gatineau, QC.

Freeman, C., Ostle, N., & Kang, H. (2001). An enzymic'latch'on a global carbon store. *Nature*, *409*(6817), 149.

Gillies, C. (2011). Water management techniques for resource roads in wetlands: A state of practice review. *FPInnovations Contract Report for Ducks Unlimited Canada CR-652*.

Graf, M. (2009). *Literature review on the restoration of Alberta's boreal wetlands affected by oil, gas and in situ oilsands development*. Ducks Unlimited Canada.

Harris, A., & Bryant, R. G. (2009). A multi-scale remote sensing approach for monitoring northern peatland hydrology: Present possibilities and future challenges. *Journal of environmental management*, *90*(7), 2178-2188.

IPCC. (2013). Technical Summary. In: *Climate Change 2013: The Physical Science Basis. Contribution of Working Group I to the Fifth Assessment Report of the Intergovernmental Panel on Climate Change.* [Stocker, T.F., Qin, D., Plattner, G.-K., Tignor, M., Allen, S.K., Boschung, J., Midgley, P.M. (eds.)]. Cambridge University Press, Cambridge, United Kingdom and New York, NY, USA. 115pp.

IPCC. (2014a). Climate Change 2014 Synthesis Report. *Contribution of Working Groups I, II and III to the Fifth Assessment Report of the Intergovernmental Panel on Climate Change* [Core Writing Team, R.K. pachauri and L.A. Meyers (eds.)]. IPCC, Geneva, Switzerland, 151 pp.

IPCC. (2014b). Drivers, Trends and Mitigation. In: *Climate Change 2014: Mitigation of Climage Change. Contribution of Working Group III to the Fifth Assessment Report of the Intergovernmental Panel on Climate Change* [Edenhofer, O., Pichs-Madruga, R., Sokona, Y., Farahani, E., Kadner, S., Seyboth, K., Minx, J.C. (eds.)]. Cambridge University Press, Cambridge, United Kingdom and New York, NY, USA.

Kang, H., Kim, S. Y., Fenner, N., & Freeman, C. (2005). Shifts of soil enzyme activities in wetlands exposed to elevated CO_2. *Science of the Total Environment*, *337*(1-3), 207-212.

Klanfar, M., Korman, T., Kujundzic, T. (2016) Fuel consumption and engine load factors of equipment in quarrying of crushed stone. *Tehnicki vjesnik* 23, 163-169, doi: 10.17559/TV-20141027115647.

Lee, Y. B., Lorenz, N., Dick, L. K., & Dick, R. P. (2007). Cold storage and pretreatment incubation effects on soil microbial properties. *Soil Science Society of America Journal*, *71*(4), 1299-1305.

Lehmann, J. R., Münchberger, W., Knoth, C., Blodau, C., Nieberding, F., Prinz, T., & Kleinebecker, T. (2016). High-resolution classification of South Patagonian Peat Bog microforms reveals potential gaps in up-scaled CH4 fluxes by use of Unmanned Aerial System (UAS) and CIR Imagery. *Remote Sensing*, *8*(3), 173.

Li, H., Zhang, L., & Shen, H. (2014). An adaptive nonlocal regularized shadow removal method for aerial remote sensing images. *IEEE Transactions on Geoscience and Remote Sensing*, *52*(1), 106-120.

Lillesand, T., Kiefer, R. W., & Chipman, J. (2014). *Remote sensing and image interpretation (6th ed.)*. John Wiley & Sons.

Liu, W., & Yamazaki, F. (2012). Object-based shadow extraction and correction of high-resolution optical satellite images. *IEEE Journal of Selected Topics in Applied Earth Observations and Remote Sensing*, *5*(4), 1296-1302.

Lovitt, J., Rahman, M.M., McDermid, G.J. (2017). Assessing the Value of UAV Photogrammetry for Characterizing Terrain in Complex Peatlands. *Remote Sensing.* 9(7). 715.

Lovitt, J., Rahman, M. M., Saraswati, S., McDermid, G. J., Strack, M., & Xu, B. (2018). UAV Remote Sensing Can Reveal the Effects of Low-Impact Seismic Lines on Surface Morphology, Hydrology, and Methane (CH4) Release in a Boreal Treed Bog. *Journal of Geophysical Research: Biogeosciences*, *123*(3), 1117-1129.

Lucieer, A., Turner, D., King, D. H., & Robinson, S. A. (2014). Using an Unmanned Aerial Vehicle (UAV) to capture micro-topography of Antarctic moss beds. *International Journal of Applied Earth Observation and Geoinformation*, *27*, 53-62.

Myhre, G., Shindell, D., Bréon, F. M., Collins, W., Fuglestvedt, J., Huang, J., ... & Nakajima, T. (2013). Anthropogenic and natural radiative forcing. *Climate change*, *423*, 658-740.

Partington, M., & Gillies, C. (2010). Resource roads and wetlands: opportunities to maintain hydrologic function. *FPInnovations Internal Report IR-2010-11-01*.

Pasher J, Seed E, Duffe J (2013) Development of boreal ecosystem anthropogenic disturbance layers for Canada based on 2008 to 2010 Landsat imagery. *Canadian Journal of Remote Sensing* 39, 42-58.

Plach, J. M., Wood, M. E., Macrae, M. L., Osko, T. J., & Petrone, R. M. (2017). Effect of a semi-permanent road on N, P, and CO2 dynamics in a poor fen on the Western Boreal Plain, Canada. *Ecohydrology*, *10*(7), e1874.

Rahman, M.M., J. Lovitt, G.J. McDermid, M. Strack and B. Xu. (2017). Mapping Peat Groundwater Table Dynamics using Unmanned Aerial Vehicle and Photogrammetric Techniques. *Remote Sensing,* 9(10), 1057.

Rahman, M. M., Hay, G. J., Couloigner, I., Hemachandran, B., Bailin, J., Zhang, Y., & Tam, A. (2013). Geographic object-based mosaicing (OBM) of high-resolution thermal airborne imagery (TABI-1800) to improve the interpretation of urban image objects. *IEEE Geoscience and Remote Sensing Letters*, *10*(4), 918-922.

Rooney, R. C., Bayley, S. E., & Schindler, D. W. (2012). Oil sands mining and reclamation cause massive loss of peatland and stored carbon. *Proceedings of the National Academy of Sciences*, *109*(13), 4933-4937.

Saha, A. K., Arora, M. K., Csaplovics, E., & Gupta, R. P. (2005). Land cover classification using IRS LISS III image and DEM in a rugged terrain: a case study in Himalayas. *Geocarto International*, *20*(2), 33-40.

Saraswati, S., Dunn, C., Mitsch, W. J., & Freeman, C. (2016). Is peat accumulation in mangrove swamps influenced by the "enzymic latch" mechanism?. *Wetlands ecology and management*, *24*(6), 641-650.

Saraswati, S., Parsons, C. T., & Strack, M. (2019). Access roads impact enzyme activities in boreal forested peatlands. *Science of the Total Environment*, *651*, 1405-1415.

Saunois, M., Jackson, R. B., Bousquet, P., Poulter, B., & Canadell, J. G. (2016). The growing role of methane in anthropogenic climate change. *Environmental Research Letters*, *11*(12), 120207.

Shi, X., Thornton, P.W., Ricciuto, D.M., Hanson, P.J., Sebestyen, S.D., Griffiths, N.A., and G. Bisht. (2015). Representing northern peatland microtopography and hydrology within the Community Land Model. *Biogeosciences*, 12, 6463-6477.

Strack, M., Waddington, J.M., Rochefort, L., and E.S. Tuitilla. (2006). Response of vegetation and net ecosystem carbon dioxide exchange at different peatland microforms following water table drawdown. *Journal of Geophysical Research*, 111, 1-10.

Strack, M., Softa, D., Bird, M., & Xu, B. (2018). Impact of winter roads on boreal peatland carbon exchange. *Global change biology*, *24*(1), e201-e212.

Tarnocai, C., Kettles, I., Lacelle, B. (2011) *Peatlands of Canada*; Geological Survey of Canada.

Tong, X., Lin, X., Feng, T., Xie, H., Liu, S., Hong, Z., & Chen, P. (2013). Use of shadows for detection of earthquake-induced collapsed buildings in high-resolution satellite imagery. *ISPRS journal of photogrammetry and remote sensing*, *79*, 53-67.

Turetsky, M. R., Kotowska, A., Bubier, J., Dise, N. B., Crill, P., Hornibrook, E. R., & Olefeldt, D. (2014). A synthesis of methane emissions from 71 northern, temperate, and subtropical wetlands. *Global change biology*, *20*(7), 2183-2197.

UNFCCC. *Adoption of the Paris Agreement*. Report No. FCCC/CP/2015/L.9/Rev.1. 2015. https://unfcc c.int/resou rce/docs/2015/cop21/eng/l09r0 1.pdf.

Vitt, D. H., Halsey, L. A., Bauer, I. E., & Campbell, C. (2000). Spatial and temporal trends in carbon storage of peatlands of continental western Canada through the Holocene. *Canadian Journal of Earth Sciences*, *37*(5), 683-693.

Yu, Z., Loisel, J., Brosseau, D. P., Beilman, D. W. & Hunt, S. J. (2010). Global peatland dynamics since the Last Glacial Maximum. *Geophysical Research Letters*, *37*(13).

Zhu, Q., Liu, J., Peng, C., Chen, H., Fang, X., Jiang, H., Zhou, X. (2014). Modelling methane emissions from natural wetlands by development and application of the TRIPLEX-GHG model. *Geoscientific Model Development,* 7, 981-999.A